IDENTIFYING ORGAN-SPECIFIC MECHANISMS TO STIMULATE LYMPHATIC GROWTH AND FUNCTION

PhD Thesis

Dániel Szőke

Molecular Medicine Doctoral School

Semmelweis University

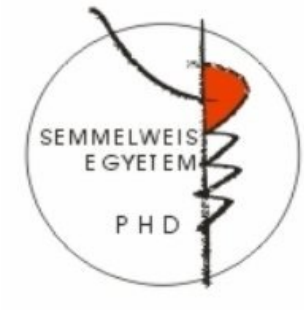

Supervisor: Zoltán Péter Jakus, MD, Ph.D

Official reviewers: Anna Horváth, MD, Ph.D
Gábor Tamás Szabó, MD, Ph.D

Head of the Complex Examination Committee:
Edit Buzás, MD, Ph.D,D.Sc, MTA lev. tagja

Members of the Complex Examination Committee:
Anna Erdei, Ph.D, D.Sc, MTA rendes tagja
Nándor Nagy, Ph.D, D.Sc

Budapest
2022

Table of Contents

List of Abbreviations

AAV – adeno-associated virus

ADAMTS3 – a disintegrin and metallopeptidase with thrombospondin motifs 3

α-SMA – alpha smooth muscle actin

B220 – B-cell marker 220

BEC – blood vascular endothelial cell

C57BL/6 – C57 black 6

CCBE1 – collagen and calcium-binding epidermal growth factor domain-containing protein 1

CD3 – cluster off differentiation 3

CD4 – cluster of differentiation 4

CD11b – cluster off differentiation 11b

CD31 – cluster of differentiation 31

CD45 – cluster of differentiation 45

CD206 – cluster off differentiation 206

Clp1 – cleavage factor polyribonucleotide kinase subunit 1

$Clp1^{K/K}$ – CLP1 kinase-dead

COVID-19 – coronavirus disease 2019

COUP TFII – chicken ovalbumin upstream promoter-transcription factor II

Cre – cyclic recombinase

DAPI – 4′,6-diamidino-2-phenylindole

DNA – deoxyribonucleic acid

EdU – 5-ethynyl-2'-deoxyuridine

ELISA – enzyme-linked immunoassay

ERK – extracellular signal-regulated kinase

ER^{T2} – eostrogen receptor type 2

FBM – fetal breathing movement

fl – floxed sequence – sequence flanked by two loxP sites

FLT4 – fms-related tyrosine kinase 4

GATA2 – GATA-binding factor 2

GFP – green fluorescent protein

GR1 – GPI-linked myeloid differentiation marker 1

HEK293T – human embryonic kidney 293T

HHEX – hematopoietically-expressed homeobox protein

iDTR – Cre-inducible diphtheria toxin receptor (human isoform of the heparin-binding EGF-like growth factor)

IQR – interquantile range

IUGR – intrauterine growth restriction

kDa – kilodalton

LNP – lipid nanoparticle

Ly6G/C (lymphocyte antigen 6 complex locus G6D/C)

LYVE1 – lymphatic vessel endothelial hyaluronan receptor 1

mRNA – messenger ribonucleic acid

Nrp2 – neuropilin 2

P – p-value, probability value

p53 – tumor protein 53

PBS – phosphate buffered saline

PCR – polymerase chain reaction

PECAM1 – platelet endothelial cell adhesion molecule 1

Poly(C) – polycytidylic acid

PROX1 – prospero homeobox 1

QPC – ubiquinone-binding protein

RDS – respiratory distress syndrome

Rh-D – rhodamine-dextran

SARS-CoV-2 – severe acute respiratory syndrome coronavirus 2

SEM – standard error of mean

SOX18 – sex determining region-box 18

T-test – Student's t-test

VEGFC – vascular endothelial growth factor C

VEGFD – vascular endothelial growth factor D

VEGFR3 – vascular endothelial growth factor receptor 3

vWF – von Willebrand factor

1. Introduction

1.1. Organ Specific Functions and Development of the Lymphatic System

The well-known classical functions of the lymphatic vessels are described as: regulation of fluid homeostasis by draining the interstitial fluid back to the blood circulation (Figure 1), absorption of lipids from the digestive system, and transportation of antigens and immune cells [1].

Novel organ-specific roles of the lymphatic system were identified lately [2, 3]. Now we know that the lymphatic system plays role in the regulation of blood pressure [4], obesity [5], cardiac growth and regeneration [6], cardioprotection of the heart after myocardial infarction [7], reverse cholesterol transport [8], regulation of the cerebrospinal homeostasis by the meningeal lymphatics [9, 10], neurodegenerative diseases [11], and preconditioning the lung for the first breaths after birth [12].

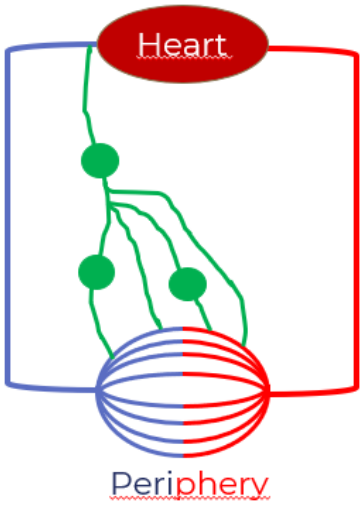

Figure 1 Main function of the lymphatic system is to drain interstitial fluid back to the circulation. Arterial side of the circulation is marked by red, venous side of the circulation is marked by blue color. Green lines mean lymphatic vessels, while green circles are lymph nodes.

Lymphatic development of the early embryonic and gestational life is well described in the literature. The lymphatic system forms after the blood circulation. Most lymphatic endothelial cells develop from blood endothelial cells of central veins after lymphatic molecular commitment [13]. These lymphatic endothelial cells form the primary lymphatic plexus from where main lymphatic collecting vessels develop. However, some lymphatic endothelial cells develop from alternative sources of origin [14, 15]. Lymphatic endothelial cells express the transcription factor PROX1 (prospero Homeobox 1) for lymphatic commitment [16], which is regulated by many transcriptional factors including: SOX18 (sex determining region Y-box 18), COUP TFII (chicken ovalbumin upstream promoter-transcription factor II), HHEX (hematopoietically-expressed homeobox protein), GATA2 (GATA-binding factor 2), fatty acid ß-oxidation, and molecules of ERK (extracellular signal-regulated kinase)-signaling route [17]. Additionally, a recent publication shows the importance of QPC (ubiquinone-binding protein) and mitochondrial complex III in lymphatic, but not in blood vessel development [18]. PROX1 itself amplifies the expression of VEGFR3 (vascular endothelial growth factor receptor 3), the main receptor for lymphatic endothelial cells [19]. VEGFC (vascular endothelial growth factor C), which is the main ligand for VEGFR3, is sufficient and essential for lymphatic vessel development [20, 21]. The VEGFC-VEGFR3 signaling route is the main signaling route for lymphatic development, maintenance and growth. VEGFC and VEGFD (vascular endothelial growth factor D) are well known ligands for VEGFR3, but VEGFC is the main physiologic lymphatic growth factor. According to the most accepted molecular model of lymphatic development, VEGFC has to be processed. The current view is that ADAMTS3 (a disintegrin and metallopeptidase with thrombospondin motifs 3) and CCBE1 (collagen and calcium-binding epidermal growth factor domain-containing protein 1) are involved in this mechanism to activate properly VEGFR3, but further studies are needed to understand the process *in vivo* [22-24]. Deletion of *Vegfc*, *Vegfr3* or *Ccbe1* is lethal in mouse models, while several point mutants of the corresponding genes result in lymphedema development and other congenital diseases in humans (e.g.: Millroy disease, Hennekam syndrome) [25, 26]. Experimental mice and clinical human data both show the importance of these genes.

All in all, although more and more roles of the lymphatic vessels are identified, more and more we know about lymphatic development in general, little is known about organ-specific functions of the lymphatics in different diseases. There is emerging data about lymphatic anatomy and function varying in different organs. Discovering organ-specific lymphatic function, and novel mechanisms in different diseases can allow us to find new specific therapeutic targets in the future.

1.2. Dysfunction of the Lymphatic System in the Skin and in the Developing Lung

1.2.1. Organ Specific Function of Lymphatic Vessels in the Skin – Lymphedema – Background, Types and Therapy

Lack or malfunction of the lymphatic vessels in skin causing lymphedema, this serious illness affects approximately 250 million people globally [27-29]. This disease results in serious reduction of quality of life, and can lead to serious infections if not treated. Still, lymphedema remains usually untreated or even undiagnosed, because of the lack of proper medical subspecialty training and clinics around the world [30]. There are two different major types of lymphedemas: primary and secondary.

Primary lymphedema is only present in around 1 of 100,000 individuals, starting generally around childhood, but can be present at any time of age [31]. Lymphedema is more frequent in females than males [32]. Primary lymphedema occurs due to genetic defects of genes which play role in lymphatic development. The most common primary lymphedemas are Hennekam syndrome (*CCBE1* gene), Milroy disease (*FLT4* (fms-related tyrosine kinase 4) gene), and Milroy like disease (*VEGFC* gene) [27].

Being the more common type, secondary lymphedema affects around 1 of 1,000 individuals and mostly people over their fifties [33]. In western countries, the most common cause of lymphedema is lymphadenectomy, or irradiation performed as breast cancer treatment. Another cause can be obstruction of lymphatic flow by tumors or other malignancies [27]. In contrast, in developing countries, around 120 million people are infected by lymphatic filariasis (caused by *Wuchereria bancrofti, Brugia malayi, Brugia timori*) which is the most common cause of lymphedema, according to the World Health Organization [34]. Other less frequent causes of secondary lymphedema are the following: venous ulcers and venous disease [35, 36], herpesvirus infection [37], and morbid obesity [38].

Nowadays there is no definitive and causative treatment for lymphedema. Current therapeutic techniques include compression therapy, physiotherapy, special dermatologic care and manual lymphatic drainage. The disease requires lifelong symptomatic treatment; therapy results only in symptomatic relief [39]. There is urgent need for a causative treatment for lymphedema. Understanding better the organ specific roles of lymphatic vessels in the skin could lead to the development of novel therapeutic techniques for this underestimated disease.

To examine organ-specific dysfunction of lymphatic vessels different lymphedema models have been developed. Most common are surgical models including surgical excision of the lymph nodes [40], ablation of the lymphatic vessels in the ear of rabbits [41, 42], tail of mice [43, 44], or hind limb of rats [45]. These models have several limitations such as low success rates, high risk of infections, the lack of standardisation. There is a great need for a reliable model to examine the effects of different therapeutic approaches on lymphedema.

Another research group suggested the use of another mouse model. Gardenier et al. set up the *Flt4-CreER^{T2}; iDTR$^{fl/fl}$* (Cre (cyclic recombinase), ER^{T2} (eostrogen receptor type 2), iDTR (Cre-inducible diphtheria toxin receptor (human isoform of the heparin-binding EGF-like growth factor), fl/fl (floxed sequence – sequence flanked by two loxP sites)) (*in vivo* genetic mouse model lately, in which Diphtheria Toxin injection resulted in local deletion of lymphatic vessels, and development of lymphedema in hind limbs of mice. Only lymphatic endothelial cells express the VEGFR3 protein in adulthood. Therefore, the *Vegfr3-CreER^{T2}* inducible system, in which the promoter region of the gene encoding VEGFR3 drives the Cre recombinase, is an efficient tool to target lymphatics [46]. The theory of the system is that if iDTR could only be expressed on lymphatic endothelial cells, then Diphtheria Toxin administration would induce the deletion of lymphatics alone. Gardenier et al. crossed *Vegfr3-CreER$^{T2;}$ iDTR$^{fl/fl}$* knock in system enabling them to induce *iDTR* expression only on the surface of lymphatic endothelial cells after gene induction. Thereafter, control solution or Diphtheria Toxin was injected into contralateral paws of *FLT4-CreER^{T2}; iDTR$^{fl/fl}$* mice. They found that lymphatic endothelial cells were deleted, lymphatic function was disrupted in the injection site and secondary lymphedema developed. The lymphedema lasted for 52 weeks [47]. This mouse model has several advantages over the abovenamed models such as more control, possibly lower infection rate, and easier standardization. That way, it can be a revolutionary method to examine organ specific function of lymphatic vessels in the skin and test new therapeutic approaches for lymphedema.

1.2.2. Lung Development and Lymphatics

One of the most difficult tasks is the adaptation to extrauterine life after birth. The opening of the fetal lung within minutes after birth is mandatory for extrauterine life. During intrauterine life, the lung is filled with amniotic fluid. Increase of compliance is a key mechanism and is mandatory for the opening of the lung during the first extrauterine breaths. Most important regulator of lung compliance is surfactant [48-50]. Lack of surfactant in the lung causes RDS (respiratory distress syndrome), that is the most common illness among premature neonates especially below 28 weeks of gestation [51]. RDS can be treated with exogenous animal surfactant administration [52], but the premature neonates still need additional supportive treatments such as oxygen administration and non-invasive or invasive ventilation leading to several complications [51, 53]. Most present animal and human studies focus on therapies related to surfactant. Studying other important mechanisms during lung development, and finding other physiological roles increasing compliance of the lung could lead to additional treatment strategies in the future.

One of the intriguing recent findings is the independent role of lymphatic vessels during lung development. Individual lymphatic endothelial cells can be found in the lung at E12.5 (embryonic day 12.5) and lymphatic vessels have been clearly formed by E14.5 in mice [54]. Jakus et al. showed that mice lacking lymphatics (CCBE1 deficient or VEGFR3 signaling deficient mouse strains) appear cyanotic and die shortly after birth due to respiratory failure. They found that anatomic changes took place, such as thickening of the alveolar septae, or reduction of the alveolar space before air inflation of the lung. Although, examined molecular or cellular mechanisms were not altered. They found that functioning lymphatic vessels are important to lung expansion and increase lung compliance during the late gestation period. The wet/dry weight ratio was increased when lymphatics were impaired. Therefore, interstitial lung edema may be the cause of lung compliance reduction [12]. Additionally, another study showed that injured pulmonary lymphatic growth resulted in reduced postnatal survival [54]. In conclusion, impaired lymphatic function results in incomplete lung development and increased occurrence of respiratory failure and mortality in newborn mice according to the abovenamed study. The question raises whether the stimulation of lymphatic function could lead to better lung development and respiratory function in newborns. Further research of lymphatics of the lung can help us better understand lung development and

result in additional therapeutic approaches for respiratory failure in newborns. But, how could we stimulate lymphatic function in the developing lung? The structure of lymphatic vessels varies depending on the location. Lymphatics in the lung have no smooth muscle coverage unlike lymphatics in other areas [55]. In adult lung the pumping mechanism of collecting lymphatic vessels is stimulated by breathing.

Similarly, late gestation embryo performs fetal breathing movements. These are periodic movements of the diaphragm performed by late gestation embryos, found in humans, large animals, and also in mice. Earlier researchers performed premature cesarean section, and examined them by plethysmography [56, 57]. Niblock et al. examined unanesthetized pregnant mice by ultrasound without opening the abdominal cavity, and showed that late gestation embryos start to perform fetal breathing movements on embryonic day 16. They had three different types: sporadic, clustered and rhythmic. The study also demonstrated an increase in the occurrence of fetal breathing movements by embryonic development [58]. Additional studies are needed to show whether these movements contribute to lymphatic drainage in the lung during late embryonic development.

1.3. Prior Approaches to Stimulate Lymphatic Function in Lymphedema and Their Limitations

According to their major role in lymphatic growth, development, and maintenance, VEGFR3 and its ligand VEGFC are ideal targets for the development of a therapeutic platform to induce regeneration and growth of lymphatic vessels in lymphedema. Besides that, such a platform could be ideal to examine the organ-specific physiological and pathophysiological functions of the lymphatic system.

There were several attempts to generate VEGFC based tools in laboratory circumstances, and use them as therapeutics to reverse experimental lymphedema. There are two major techniques in the literature for VEGFC administration: protein or adenovirus/ adeno-associated virus based vector systems [59].

Protein administration has major disadvantages such as the high cost and difficult techniques of production, the complex methods for purification and the problem of maintenance of a long-lasting effect is still not solved [60].

There were several attempts to grow or even regenerate lymphatic vessels by administration of VEGFC as recombinant protein, but these previously promising attempts only had limited effects [7, 11, 61-64].

Szuba and colleagues needed high dose, 100 μg of human recombinant VEGFC protein to induce lymphangiogenesis, and treat postsurgical lymphedema in ears of rabbits [61]. Jin and coworkers showed lymphatic vessel growth and positive remodeling after VEGFC administration in murine tail lymphedema model [64]. Another research group tried to regrow lymphatic collecting vessels after performing full-dermis thickness incisional wound and injecting 200 ng of VEGFC protein. Although, all measured lymphatic parameters were significantly increased after VEGFC injection compared to controls, and lymphangiogenesis near the wound was more common, these differences were not significant. Furthermore, there were no changes in the clinical aspects of the wound (e.g., edema) [62]. Because of the minimal short-acting effect, some research groups used albumin-alginate microparticle or hydrogel bound forms of VEGFC to lengthen and regulate the effect in the meningeal compartment or in heart after myocardial surgery in rats [7, 11].

Another technique used to administer VEGFC in the literature are adenovirus and adeno-associated virus-based systems. Adenovirus and adeno-associated virus-based systems of VEGFC were an effective way to stimulate lymphatic growth in mice and pigs. Also, a drug candidate entered a Phase II clinical trial (NCT03658967) [22, 65-73]. Although these techniques made continuous and regulated protein expression possible, they have other serious potential downsides. The use of these virus vector-based systems can result in genome integration. Regulation of the possible expression amplification is not solved, and the vector virus itself can cause immune reactions and vascular growth. Furthermore, potential carcinogenic effect was also described [74, 75].

1.4. Novel in Vivo Protein Expression System for Vaccine Development: Nucleoside Modified mRNAs Encapsulated into Lipid Nanoparticles

Nucleoside modified mRNA-LNP (mRNA (messenger ribonucleic acid), LNP (lipid nanoparticle)) system (Figure 2) is a novel approach for protein expression *in vivo* invented for vaccine development against viral infections such as: influenza, rabies and Zika virus [76-82]. Its importance was recognized during the COVID-19 (coronavirus disease 2019) pandemic, when mRNA-LNP vaccines were used for the first time as human therapeutics. Multiple manufacturers produced vaccines utilizing this method and studying them in Phase III clinical trials during the COVID-19 pandemic. Based on these studies and numerous publications, the currently developed mRNA-LNP vaccines are efficient, and they barely have any side effects [83, 84]. This technology has also promising potential in other medical fields such as cancer therapy [80, 85], therapeutic protein expression or replacement [86-89], and gene editing [90]. Before mRNA technology could be a highly functioning system, researchers had to overcome obstacles such as: instability, innate immune reactions and inefficient *in vivo* delivery. Nucleoside modification of mRNAs and encapsulation of mRNAs into lipid nanoparticles, which is a newly developed drug delivery system, helped mRNA therapy not just to be delivered easily to cells but to be more stable and hidden from the innate immune system.

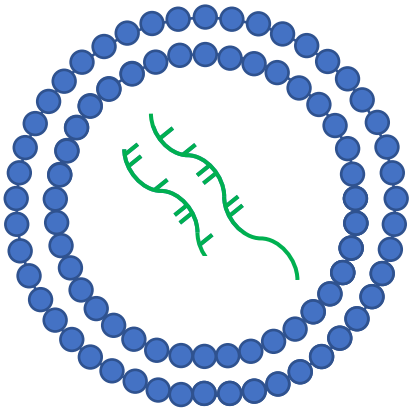

Figure 2 Schematic Structure of the mRNA-LNP System. The mRNAs (green objects) are incorporated into a double lipid layer structure (blue dots), which is called lipid nanoparticle. It contains several different lipid molecules.

mRNA techniques are not just excellent therapeutics, but more advantageous compared to other *in vivo* protein expression systems such as adenovirus or adeno-associated virus ones. There is no possible integration into the host DNA (deoxyribonucleic acid), no anti-vector immunity or innate immune activation, yet the protein production is long lasting and easily controllable. Last but not least the *in vitro* transcription of the mRNA is a simpler and easier task than vector generation or protein production and purification [77].

All in all, nucleoside modified mRNA encapsulated into lipid nanoparticles is a promising technology not just for vaccine development, but also for *in vivo* protein expression. It might be an excellent way to induce the production of VEGFC, lymphatic growth, function, and to study the organ-specific role of lymphatics.

1.5. Past Animal Studies of Fetal Breathing Movements in Lung Development

Several studies showed that fluid secretion and mechanical forces are the key regulators for embryonic lung development [91-95]. Fetus performs periodic breathing-like movements called fetal breathing movements during late gestation, which generate mechanical forces. Researchers tried to examine mechanical forces and FBMs (fetal breathing movement) during lung development *in vivo* in the past with three different methods: heroic surgical methods, anhydramnios models and paralysis causing mutation models.

Some researchers tried to induce the absence of late gestation FBMs by heroic surgical interventions. Intrauterine surgical methods were used such as phrenic nerve section and spinal cord transection in lamb fetuses to examine the role of FBMs [96, 97]. These surgical interventions resulted in reduced lung expansion and reduced wet lung weight. Authors concluded upon these findings that absence of FBMs results in lung hypoplasia. But detailed analysis of the data shows that the dry weight of the lung was not altered which indicates that lung hypoplasia did not develop. When other researchers repeated the experiment in a sham-controlled study, they found that the histological and wet weight findings were even more explicit in the control animals than in the studied ones. In conclusion in this study it was found that the lack of FBMs might be responsible for lung hypoplasia [98].

Others drained the amniotic fluid in animal studies, which resulted in absence of FBMs. This model is related to the clinical observation which show that in anhydramnios, when amniotic fluid is fully leaked, the lung is collapsed. Unfortunately, lung hypoplasia is also

present in this condition. A research group showed permanent amniotic fluid leakage resulting in atelectasis in the lung and lung hypoplasia. This model has several limitations, the absence of amniotic fluid results in the absence of FBMs, but also affects development of the fetus [91].

Third type of experimental method used to eliminate FBMs is based on the clinical observation, that skeletal muscle development disorders result in altered lung development, referred to as lung hypoplasia [99]. Unfortunately, these human fetuses have IUGR (intrauterine growth restriction), suggesting that early movements and the muscle innervation are also important for skeletal development. Related to this observation, in one study authors observed mouse fetuses in which a genetic mutation caused paralysis from the start of gestation. They found not only lung hypoplasia but also the reduction of the overall embryonic weight like in skeletal muscle development disorders. Biggest limitation of this study is that not only the FBMs were affected, because the muscles were paralyzed from the early period of embryonic life. This way the dysmature phenotype and lung hypoplasia can be a result of overall skeletal developmental problem and not the lack of FBMs [100].

All of these animal models have great limitations and they could not examine FBMs or mechanical forces in the developing lung alone so there is a great need for a better animal model to understand the roles of FBMs in lung development.

One important question can be, what kind of animals should one use to study FBMs. A recently published article showed the presence of FBMs with ultrasound technique in unanesthetized pregnant mice. They found that the development of FBMs start at embryonic day 16 and showed rigorously the development and changes of FBMs during embryonic life of the fetuses [58].

How can FBMs be related to lymphatic vessels? It is important to note that collecting lymphatic vessels have smooth muscle coverage to introduce pumping function and lymphatic fluid flow in most of organs [101], but in contrast to that collecting lymphatic vessels in the lung lack this smooth muscle coverage [55]. Thus, it is a logical theory that another mechanism is important for the lymphatic flow. In adults the permanent periodic breathing can assist to that as a natural pumping mechanism, but it is not present in the developing lung.

1.6. Novel Genetic Model for Late Gestational Neuronal Degradation

The *Clp1*$^{K/K}$ *(cleavage factor polyribonucleotide kinase subunit 1)* mouse model is a promising mouse model, which could be used for examining the FBMs. Recently a research group showed that *Clp1*$^{K/K}$ late gestation embryos lose innervation of skeletal muscles via a progressive axonal degeneration mechanism. The loss of CLP1 kinase activity results in small RNA fragment accumulation in the neurons because of aberrant processing of pre-transfer RNAs. As the research group showed, the reexpression of wild type CLP1 or genetic inactivation of p53 (tumor protein 53) rescues the motoneuron loss, so this is a p53-dependent process.

The degeneration starts from 16.5 days of gestation, that is exactly the time point when FBMs appear. Thus, it can be an ideal platform to examine the absence of FBMs alone without affecting early skeletal and muscle development [102].

FBMs can be one potential pumping mechanism of the lymph flow, because collecting lymphatic vessels lack smooth muscle coverage in the lung. *Clp1*$^{K/K}$ model can be a promising model to study not just the lack of FMBs, but also the organ-specific lymphatic function in the developing lung.

2. Objectives

To understand better the organ-specific physiological and pathophysiological roles of the lymphatics in the skin and in the developing lung, which can potentially lead us to better therapeutic approaches against secondary lymphedema in adult patients and respiratory failure in newborns.

To examine organ-specific function of lymphatics in the skin, we wanted to develop a novel nucleoside-modified VEGFC mRNA platform (VEGFC mRNA-LNP) to induce organ-specific lymphatic growth *in vivo* including the following steps:

- development and production of the VEGFC mRNA-LNP platform;
- characterization of the VEGFC mRNA-LNP system *in vitro;*
- characterization of the VEGFC mRNA-LNP system *in vivo;*
- testing the VEGFC mRNA-LNP complexes in an experimental lymphedema mouse model *in vivo.*

To better understand physiologic and pathophysiologic roles of the lymphatics in the developing lung we aimed the followings:

- setting up a mouse model, in which FBMs are impaired during late gestation embryonic development;
- characterizing the phenotype of $Clp1^{K/K}$ newborn mice;
- setting up an ultrasound-based system to monitor FBMs;
- monitoring the FBMs in $Clp1^{K/K}$ and control embryos during development *in utero.*

3. Results

3.1. VEGFC Protein Is Present in the Supernatant of HEK293T Cells After VEGFC mRNA-LNP Transfection

First, murine VEGFC-encoding 1-methylpseudouridine-containing mRNAs were designed, synthetized, purified, and encapsulated into LNPs in cooperation with Dr. Norbert Pardi from the University of Pennsylvania and Acuitas Therapeutics in Canada.

For the first analysis VEGFC mRNA-LNPs were tested in an *in vitro* experiment. 1 µg of Poly(C) RNA-LNPs or VEGFC mRNA-LNPs were added to the medium of HEK293T (human embryonic kidney 293T) cells. 8 hours, 1, 4, 8 days after the treatment the supernatant of the cells was harvested. 4 and 8 days after the transfection VEGFC protein were present and detectable with Western Blot analysis (Figure 3).

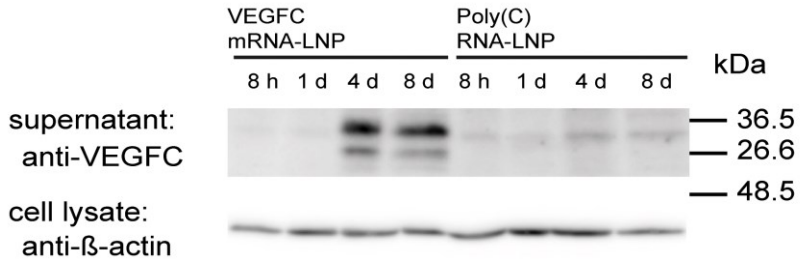

Figure 3 Administration of VEGFC mRNA-LNPs Induces VEGFC Secretion *in Vitro.* "1 µg of Poly(C) or VEGFC mRNA-LNPs were added to the medium of HEK293T cells, and VEGFC (in supernatants) and β-actin (in cell lysates) protein expression levels were determined at 8 hours and at days 1, 4, 8 by Western blot analyses. Representative images are shown of 3 independent experiments." [I]

3.2. VEGFC Protein Is Expressed in Vivo Locally After VEGFC mRNA-LNP Administration

Then, *in vivo* effects of VEGFC mRNA-LNP injection were examined. After VEGFC mRNA-LNP injection into one ear of a wild type C57BL/6 (C57 black 6) mice, higher levels of VEGFC protein were measured in the interstitial fluid of the ear compared to the contralateral side injected with Poly(C) (polycytidylic acid) RNA-LNP as control. The elevated VEGFC protein level was present and significant on 1, 5, 10 and 15 days after the injection. On the twentieth day minimal elevation was present but was not significantly higher (Figure 4).

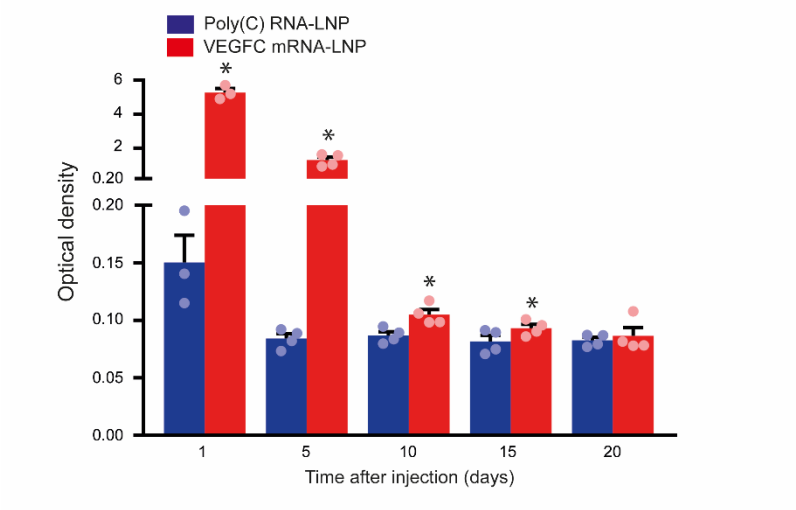

Figure 4 Administration of VEGFC mRNA-LNPs Induces VEGFC Secretion *in Vivo.* "1 µg of Poly(C) or VEGFC mRNA-LNPs were injected into contralateral ears of mice intradermally. Interstitial fluid samples were harvested 1, 5-, 10-, 15- and 20-days post injection and VEGFC protein expression levels were determined by ELISA (enzyme-linked immunoassay). Quantitative data for the secreted amount of VEGFC are represented as mean and SEM (standard error of mean) from Poly(C) or VEGFC mRNA-LNP injected ears of 3–4 mice at each time point (two-tailed, paired T-test (Student's t-test), $P = 0.0023$ (p-value, probability value) after 1 day for 3 mice, $P = 0.0063$ after 5 days for 4 mice, $P = 0.0017$ after 10 days for 4 mice, $P = 0.0332$ after 15 days for 4 mice, and $P = 0.7025$ after 20 days for 4 mice). Asterisks indicate $P < 0.05$ compared with control." [I]

3.3. Organ-Specific Lymphatic Growth Is Present After VEGFC mRNA-LNP Injection

Secondly, lymphatic morphology was assessed. One ear of *Prox1*^{GFP} mice was injected with VEGFC mRNA-LNP complexes and the other ear was treated with Poly(C) RNA-LNP as control. Lymphatic endothelial cells of *Prox1*^{GFP} mice express GFP (green fluorescent protein) so it is an excellent tool to assess lymphatic morphology. LYVE1 (lymphatic vessel endothelial hyaluronan receptor 1) is an excellent marker for staining lymphatic endothelial cells.

22 days and 60 days after VEGFC mRNA-LNP administration, significant lymphatic growth was detected in ears (Figure 5). Quantification of the data showed significant increase in the length of the lymphatic network, the average diameter of lymphatic vessels and the number of branching points after 5, 12, 17, 22, 35 and even after 60 days (Figure 6). We also detected a dose dependent lymphatic growing effect. (To that end, we performed two-way ANOVA in all cases. In the case of length of the lymphatic network: factor P = 0.0003. According to the post-hoc analysis between doses 0.04 µg vs. 0.2 µg of VEGFC mRNA-LNP injection P = 0.6025, 0.04 µg vs. 1 µg P = 0.0001, 0.2 µg vs. 1 µg P = 0.0016. In the case of average diameter of lymphatics: factor P = 0.6236. According to the post-hoc analysis between doses 0.04 µg vs. 0.2 µg of VEGFC mRNA-LNP injection P = 0.9873, 0.04 µg vs. 1 µg P = 0.4642, 0.2 µg vs. 1 µg P = 0.6801. In the case of average branching points / field of view: factor P = 0.0003. According to the post-hoc analysis between doses 0.04 µg vs. 0.2 µg of VEGFC mRNA-LNP injection P = 0.0169, 0.04 µg vs. 1 µg P < 0.0001 0.2 µg vs. 1 µg P = 0.381.) Additionally, Significant increase of all three morphology parameters were observed when injected with as low as 0.04 µg (Figure 7).

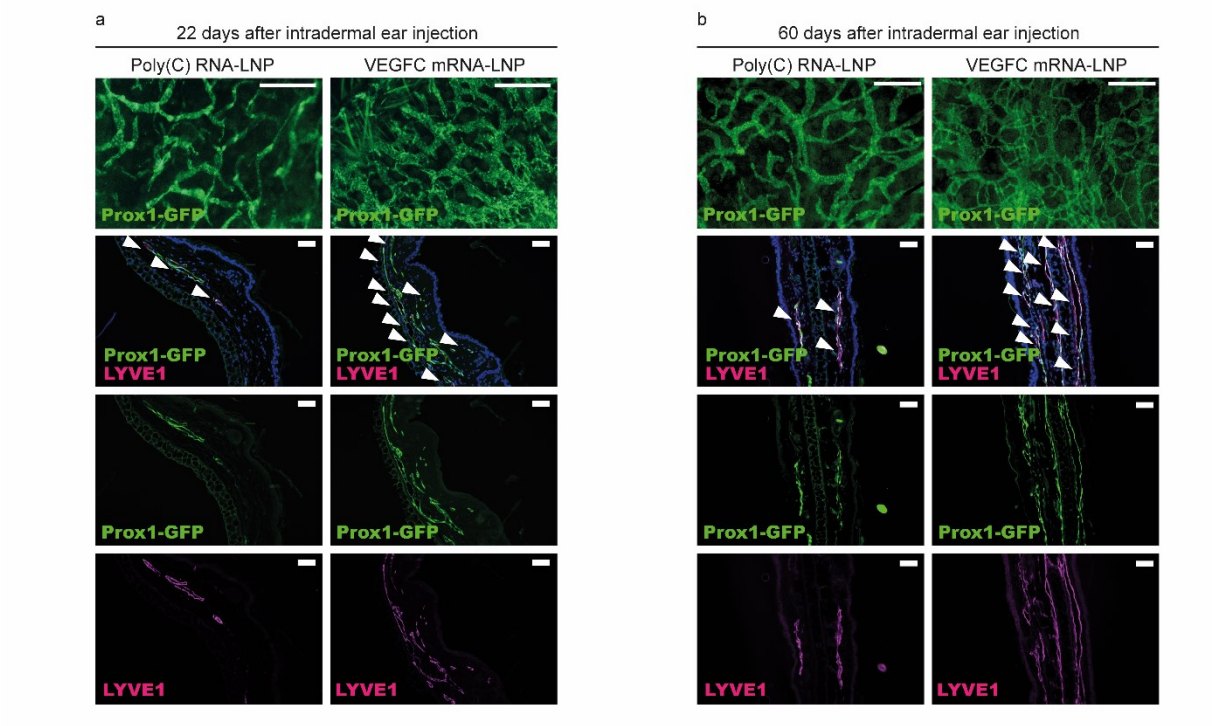

Figure 5 Administration of VEGFC mRNA-LNPs Induces Local Lymphatic Growth in Mice *in Vivo*. „**(a–b)** Analysis of lymphatic morphology in the ear of Prox1^{GFP} lymphatic reporter mice injected with 1 µg of Poly(C) or VEGFC mRNA-LNPs. Representative images 22 days **(a)** and 60 days **(b)** after the treatment of ear of 15 **(a)** and 5 **(b)** mice in each group are shown by whole-mount fluorescent stereo microscopy (upper panels; bars: 1000 µm **(a)** and 500 µm **(b)**) and Prox1^{GFP} signal and LYVE1 are shown by anti-LYVE1 immunostaining of slides processed by paraffin-based histology (lower panels; bars: 50 µm). Arrows indicate Prox1^{GFP} and LYVE1 double positive lymphatic vessels." [I]

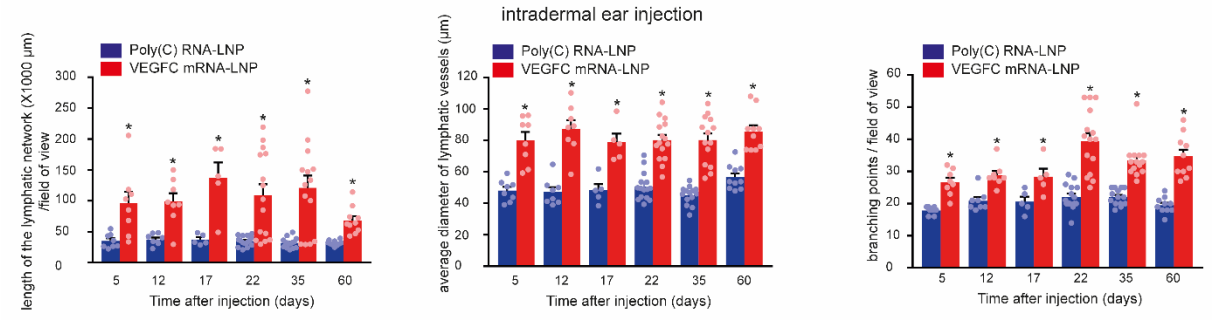

Figure 6 Time Dependency of VEGFC mRNA-LNP Injection Induced Local Lymphatic Growth in Mice *in Vivo*. "Assessment of the time-dependent effect of intradermal administration of 1 µg of Poly(C) or VEGFC mRNA-LNPs in the ear at days 5, 12, 17, 22, 35 and 60. Quantitative data for the length of lymphatic network, average lymphatic vessel diameter and number of branching points per vision field are represented as mean and SEM from Poly(C) or VEGFC mRNA-LNP-injected ears of 5-15 mice in each group (two-tailed, paired T-test, for lymphatic network length P = 0.0005 after 22 days for 15 mice and P = 0.0005 after 60 days for 10 mice. For average lymphatic vessel diameter P = 0.000005 after 22 days for 15 mice and P = 0.0002 after 60 days for 10 mice. For number of branching points P = $7.48*10^{-7}$ after 22 days for 15 mice and P = 0.0001 after 60 days for 10 mice)." [I]

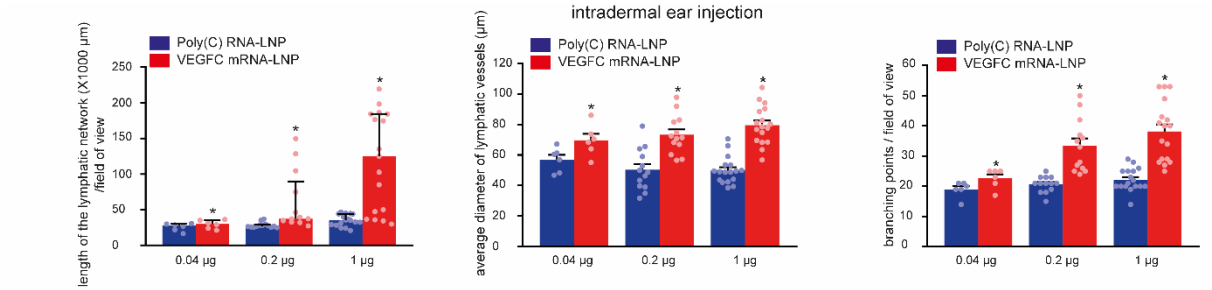

Figure 7 Dose-Dependency of Lymphatic Morphology Parameters of Mice Injected with VEGFC mRNA-LNPs. "Monitoring the dose-dependent effect of Poly(C) or VEGFC mRNA-LNPs (0.04, 0.2 and 1 µg) 20 days after intradermal treatment of the ear. Quantitative data for the length of lymphatic network, average lymphatic vessel diameter and number of branching points per vision field are represented as mean and SEM from LNP complex-injected ear of 6-17 mice in each group (two-tailed Wilcoxon signed-rank test for lymphatic network length P = $7.04*10^{-5}$ for 17 mice, two-tailed, paired T-test for average lymphatic vessel diameter P = $4.61*10^{-7}$ for 17 mice and two-tailed, paired T-test for number of branching points P = $6.84*10^{-7}$ for 17 mice when injected with 1 µg of Poly(C) or VEGFC mRNA-LNP)." [I]

We also investigated the effect of VEGFC mRNA-LNP on lymphatics in other organs to show the versatility of this platform. We observed increased lymphatic growth in the diaphragm after intraperitoneal, in the lung after intratracheal, and in the gastrocnemius muscle after intramuscular injection of the VEGFC mRNA-LNP compared to control solution. Quantification of histology slides stained with LYVE1 and Podoplanin lymphatic specific markers showed significant increase in the number of lymphatic vessels (Figure 8).

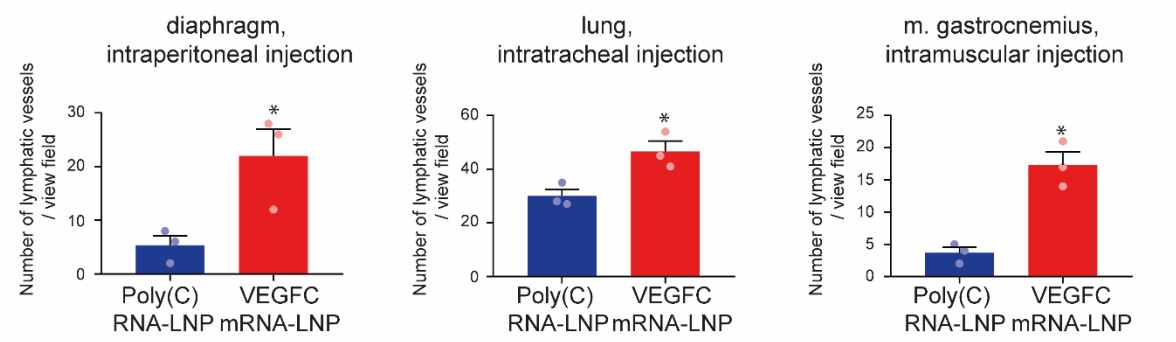

Figure 8 Administration of VEGFC mRNA-LNPs Into Variable Organs Induces Local Lymphatic Growth in Diaphragm, Lung and Gastrocnemius Muscle in Mice in Vivo. "Monitoring the effect of 1 µg locally injected Poly(C) or VEGFC mRNA-LNPs on lymphatic growth in *Prox1*^{GFP} mice in the diaphragm 22 days after intraperitoneal injection, in the lungs 22 days after intratracheal treatment, and in the musculus gastrocnemius 22 days after intramuscular injection. Quantitative data for number of the lymphatics are shown as mean and SEM of Poly(C) or VEGFC mRNA-LNP-injected organs of 3 mice in each group. Asterisks indicate $P < 0.05$ compared with control (two-tailed, unpaired T-test, diaphragm: $P = 0.0354$ for 3 mice, lung: $P = 0.0222$ for 3 mice, two-tailed, paired T-test m. gastrocnemius: $P = 0.0145$ for 3 mice)." [I]

We performed the so called EdU proliferation assay. EdU (5-ethynyl-2′-deoxyuridine) is a thymidine analogue so it incorporates into DNA of proliferating cells. EdU was administered 5 days after Poly(C) or VEGFC mRNA-LNP treatment of animals, then they were terminated 24 hours thereafter. EdU+ and LYVE1+ proliferating lymphatic endothelial cells and the mitotic index were quantified and calculated from immunohistochemistry images of paraffin-based sections. The number and percentage of EdU positive nuclei of lymphatic endothelial cells were increased in ears injected with 1 µg of VEGFC mRNA-LNP compared to the Poly(C) mRNA-LNP injected ones shown by fluorescent and confocal microscopy (Figure 9).

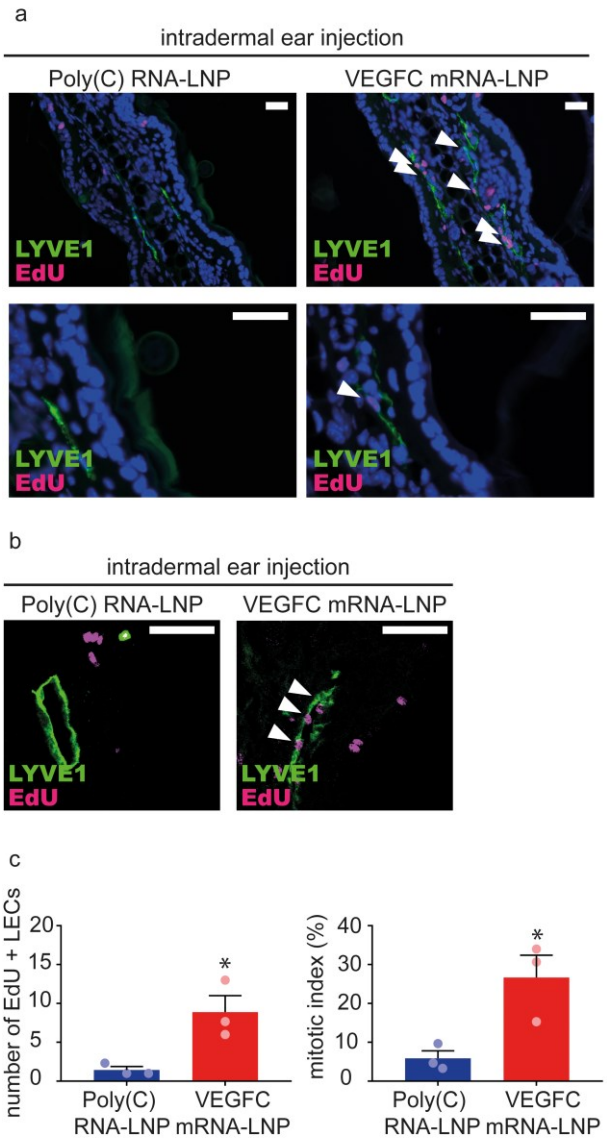

Figure 9 Administration of VEGFC mRNA-LNPs Induces Local Lymphatic Proliferation in Mice in Vivo. "**(a–b)** Assessment of lymphatic proliferation 5 days after intradermal injection with 1 µg of Poly(C) or VEGFC mRNA-LNPs. EdU staining and anti-LYVE1 immunostaining of slides processed by paraffin-based histology (bars, 50 µm) shown by widefield **(a)** and confocal imaging **(b)**. Arrows indicate EdU and LYVE1 double positive lymphatic endothelial cell nuclei. Representative images of 3 ears of 3 mice in each group are shown. **(c)** Number of EdU positive lymphatic endothelial cells (two-tailed, unpaired T-test, P = 0.0260 for 3 mice) and mitotic index (two-tailed, unpaired T-test, P = 0.0266 for 3 mice) are shown 5 days after intradermal injection with 1 µg of Poly(C) or VEGFC mRNA-LNPs. Quantitative data for lymphatic proliferation are represented as mean and SEM from 3 injected ears of 3 mice in each group." [I]

3.4. No Adverse Effect Was Observed After VEGFC mRNA-LNP Injection

To assess the possible side effects of VEGFC mRNA-LNP injection, we performed further experiments. First, we examined the possible off target effects in other organs. Second, we assessed blood vessel growth. Third, immune response was investigated.

For organ specificity studies, *Prox1*^{GFP} transgenic mice – where lymphatic endothelial cells express GFP – were injected with Poly(C) or VEGFC mRNA-LNP into the ears. The injected ears, contralateral ears, lungs and small intestines of Prox1^{GFP} animals were collected 22 days after injection, and GFP^{+} cells were quantified using flow cytometry. Significant increase in the number of GFP^{+} cells was found in the injected organ, but no difference was observed in other organs (Figure 10).

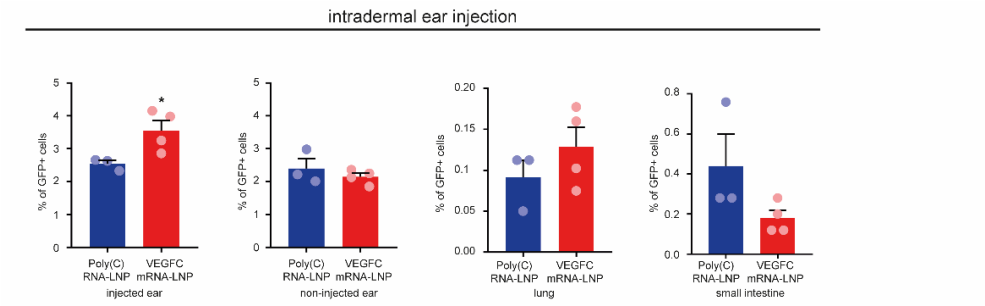

Figure 10 Administration of VEGFC mRNA-LNPs Results in Organ-Specific Effects in Vivo. "Monitoring the effect of intradermal injection into ears of Prox1^{GFP} mice with 5 µg of Poly(C) or VEGFC mRNA-LNPs shown by flow cytometry analysis. 5 µg of Poly(C) or VEGFC mRNA-LNPs were intradermally injected into the ear. Injected and non-injected ears, lungs, and small intestines were harvested and digested into single cell suspension. Quantitative data for GFP positive cell number are represented as mean and SEM from Poly(C) or VEGFC mRNA-LNP-injected ears, non-injected ears, non-injected lungs, and non-injected small intestines of 4 mice in VEGFC mRNA-LNP group and 3 mice in the control group 22 days after mRNA-LNP injection (two-tailed, unpaired T-test for injected ears of Poly(C) RNA-LNP injected vs VEGFC mRNA-LNP injected mice $P = 0.0402$, two-tailed, unpaired T-test for contralateral non-injected ears of Poly(C) RNA-LNP injected vs. VEGFC mRNA-LNP injected mice $P = 0.4006$, two-tailed, unpaired T-test for lungs of Poly(C) RNA-LNP injected vs VEGFC mRNA-LNP injected mice $P = 0.3168$, two-tailed, unpaired T-test for small intestines of Poly(C) RNA-LNP injected vs VEGFC mRNA-LNP injected mice $P = 0.1252$). Asterisks indicate $P < 0.05$ compared with control." [I]

As it was reported in previous studies, the virus vector-based administration of proteins can result in significant immune response and blood vessel proliferation [103, 104]. In contrast, one study showed no significant immune response after nucleoside modified mRNA-LNP injection [79]. Therefore, we examined the possible side effects of the VEGFC mRNA-LNP system such as, blood vessel proliferation or immune cell infiltration.

To examine the possible blood vessel proliferation, Poly(C) or VEGFC mRNA-LNP was injected into ears of mice. We found no significant difference in the number of blood vessels between Poly(C) RNA-LNP and VEGFC mRNA-LNP injected groups shown by CD31 (cluster of differentiation 31) and vWF (von willebrand factor) immunostaining 22 days after injection. CD31 is present on both lymphatics and blood vessels for it is a panendothelial marker. vWF can only be detectable on blood endothelial cells thus antibodies against it stain only blood vessels. In contrast, the increase of lymphatic vessel number was present as shown by LYVE1 and Podoplanin immunostaining (Figure 11a and b).

To assess the possible immune cell infiltration, previously Poly(C) or VEGFC mRNA-LNP treated ears of *Prox1*^{GFP} mice were digested, then flow cytometry analysis was made against LYVE1 – to assess lymphatic endothelial cell number – or different immune cell specific markers such as: CD45 (cluster of differentiation 45) for all immune cells, Ly6G/C ((lymphocyte antigen 6 complex locus G6D/C) (GR1 (GPI-linked myeloid differentiation marker 1)) for neutrophil granulocytes, CD206 (cluster of differentiation 206) for macrophages and dendritic cells, CD3 (cluster of differentiation 3) for T cells, B220 (B cell marker 220) for B cells, and CD11b (cluster of differentiation 11b) for monocytes and many other immune cells. We made certain that we show only CD11b+ Ly6G/C- cells hence neutrophils are not gated again. There were significantly more lymphatic endothelial cells in the VEGFC mRNA-LNP treated ears compared to the controls, but there was no significant difference when the number of any assessed immune cells were compared (Figure 12).

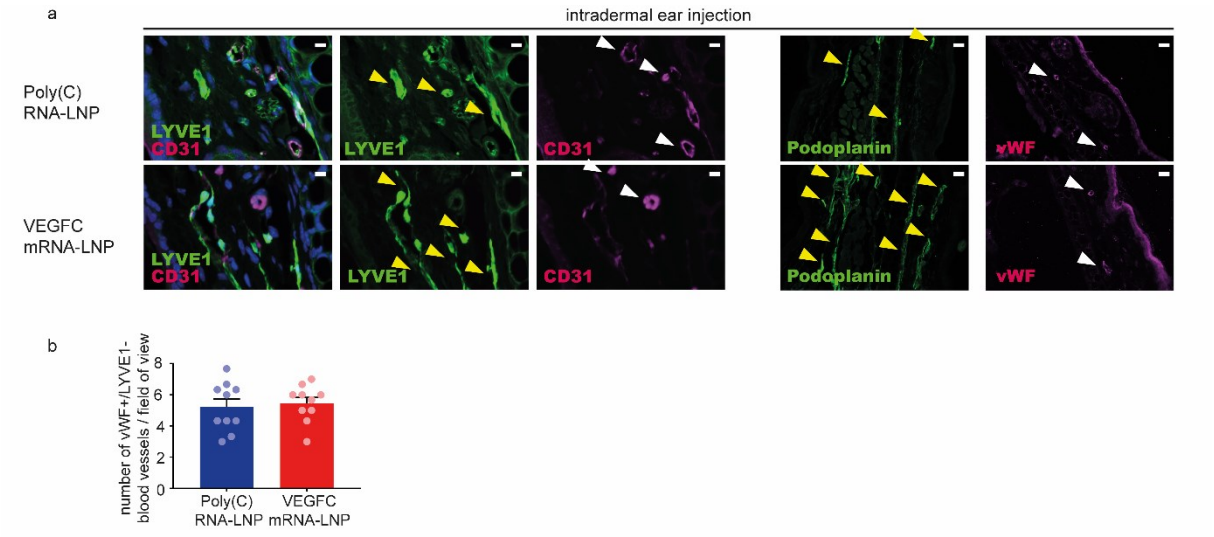

Figure 11 Administration of VEGFC mRNA-LNPs Results in No Blood Vessel Proliferation. "**(a)** 1 µg of Poly(C) or VEGFC mRNA-LNPs was intradermally injected into the ear of C57BL/6 mice and the growth of blood and lymphatic vessels were examined 22 days after the injection. Representative images of anti-CD31, anti-LYVE1, anti-Podoplanin, and anti-vWF stained paraffin-embedded ear samples are shown of 5 mice in each group (bars, 25 µm (anti-CD31, anti-LYVE1), 50 µm (anti-Podoplanin, anti-vWF)). Yellow arrows indicate LYVE1 positive lymphatic vessels, white arrows indicate CD31 positive and LYVE1 negative blood vessels. (**b)** The number of vWF high and LYVE1 negative blood vessels was determined 22 days after the administration of 1 µg of Poly(C) or VEGFC mRNA-LNPs. Data are represented as mean and SEM from slides of ears of 10 mice per group (two-tailed, paired T-test, P = 0.6344 for 10 mice)." [I]

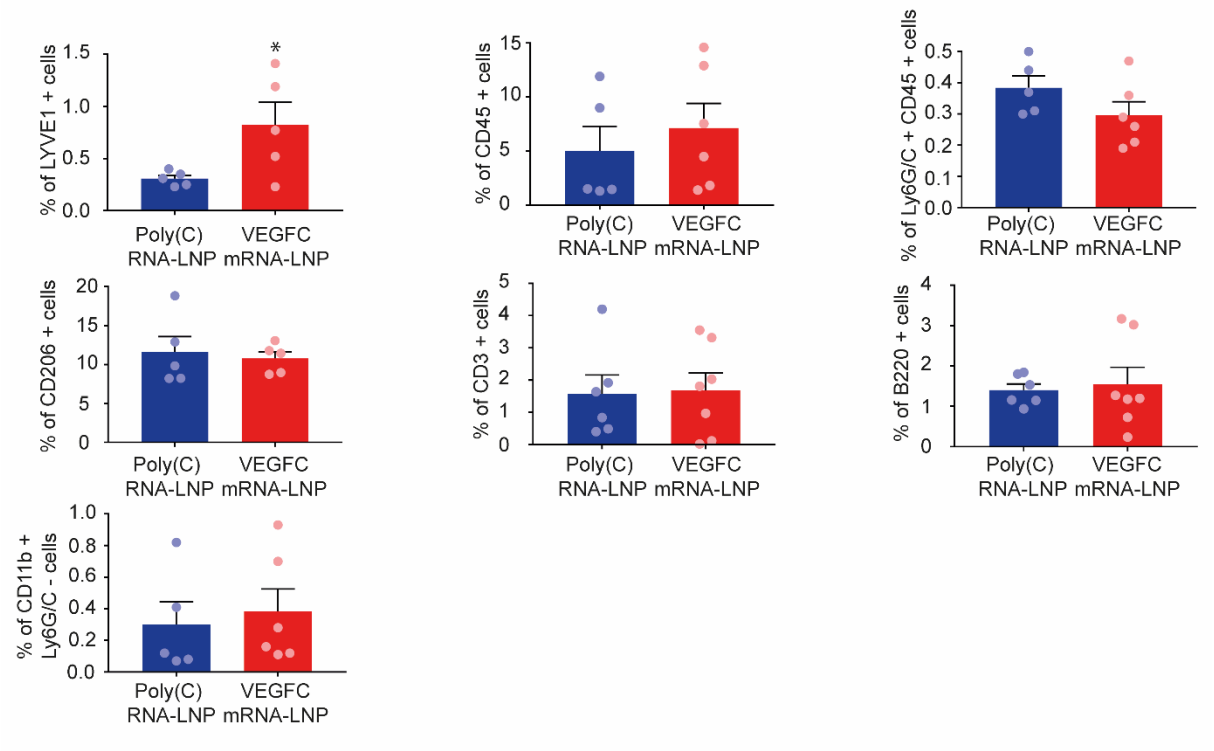

Figure 12 VEGFC mRNA-LNP Injection Results in No Significant Immune Response Activation. "Monitoring the effect on lymphatic endothelial cells and immune cells after intradermal injection of 1 µg of Poly(C) or VEGFC mRNA-LNPs into ears of Prox1^{GFP} mice shown by flow cytometry analysis. Quantitative data for LYVE1+, CD45+, Ly6G/C+, CD206+, CD3+, B220+, CD11b+ and Ly6G/C- cell numbers are represented as mean and SEM from Poly(C) or VEGFC mRNA-LNP-injected ears of 5–7 mice in each group, 22 days after mRNA-LNP injection (two-tailed, unpaired T-test, P = 0.0450 for LYVE1+ for 5 mice injected with Poly(C) and for 5 mice injected with VEGFC mRNA-LNP, P = 0.5365 for CD45+ for 5 mice injected with Poly(C) and for 6 mice injected with VEGFC mRNA-LNP, P = 0.1689 for Ly6G/C+ and CD45+ for 5 mice injected with Poly(C) and for 6 mice injected with VEGFC mRNA-LNP, P = 0.7211 for CD206+ for 5 mice injected with Poly(C) and for 5 mice injected with VEGFC mRNA-LNP, P = 0.8947 for CD3+ for 6 mice injected with Poly(C) and for 7 mice injected with VEGFC mRNA-LNP, P = 0.7748 for B220+ for 6 mice injected with Poly(C) and for 7 mice injected with VEGFC mRNA-LNP and P = 0.6922 for CD11b+ Ly6G/C- for 5 mice injected with Poly(C) and for 6 mice injected with VEGFC mRNA-LNP comparing cell number)." [I]

3.5. Newly Grown Lymphatic Vessels Induced by VEGFC mRNA-LNP Are Fully Functional

Although our results show that lymphatic vessels induced by VEGFC mRNA-LNP appear to have normal morphology, we performed a number of additional experiments to examine the functionality of these newly formed lymphatic vessels.

70 kDa (kilodalton) Rh-D (Rhodamine-dextran) is a specific and efficient tool to examine lymphatic function. The interstitially injected macromolecules can be taken up and transported by lymphatics but not by the blood vessels. Thus, we injected fluorescently labeled macromolecules to make lymphatic function visible.

In our experiments Poly(C) RNA-LNP was injected to one and VEGFC mRNA-LNP to the contralateral ear of *Prox1*^{GFP} mice. 70 kDa Rhodamine-dextran was injected into both ears 22 days after the treatment. Fluorescent images were made by stereo microscopy. The green signal of Prox1^{GFP} and the magenta signal of the macromolecules were overlapping which indicated that the lymphatic vessels took up and transported the macromolecules (Figure 13).

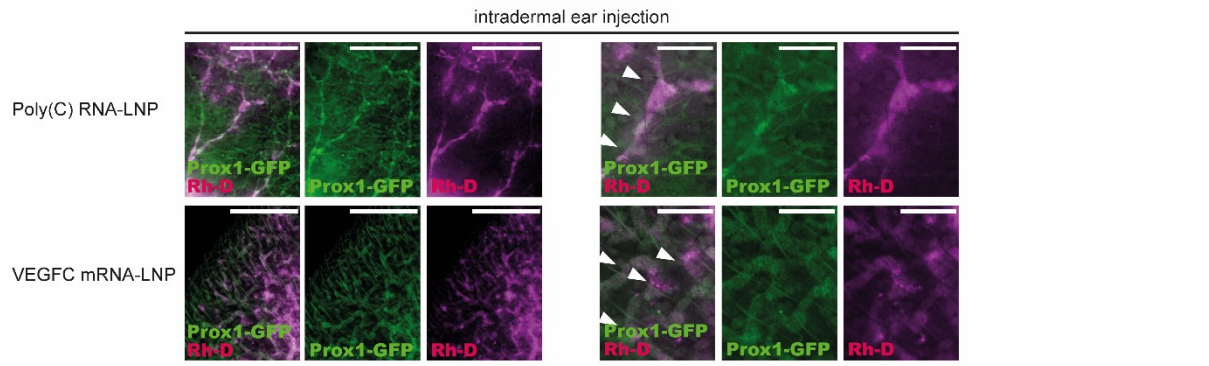

Figure 13 Administration of VEGFC mRNA-LNPs Stimulates Active Lymphatic Function. "Monitoring active lymphatic function in the ears of Prox1^{GFP} mice after intradermal injection of 1 µg of Poly(C) or VEGFC mRNA-LNPs. Twenty-two days after treatment, 70 kDa Rh-D was injected into the ear and the transport of the molecule was monitored by fluorescent microscopy 60 min post Rh-D administration. Representative images are shown of 10 injected mouse ears per group, figures on the right are zoomed in images (bars, 1000 µm left, 385 µm right). Arrows indicate Prox1-GFP positive and Rh-D positive lymphatic vessels." [I]

3.6. Application of an in Vivo Genetic Model to Induce Experimental Lymphedema in Mice

To examine the effect of VEGFC mRNA-LNP injection on lymphedema and demonstrate the proof-of-concept in a disease model we set up the *Flt4-CreER^{T2}; iDTR$^{fl/fl}$ in vivo* genetic mouse model in which Diphtheria Toxin injection results local deletion of lymphatic vessels and development of lymphedema.

Thickening and swelling of the paws and elevation of clinical score peaked 8 days after the first Diphtheria Toxin injection and this effect was present until up to 60 – in the case of clinical score – and to 75 days – in the case of width – post injection (Figure 14a). To examine the histological changes specific to secondary lymphedema, we stained sections prepared from treated limbs with Hematoxylin and Eosin which showed the increase of fibroadipose area in Diphtheria Toxin treated paws (Figure 14b, c). Fluorescent immunohistochemistry against lymphatic vessel specific markers such as, LYVE1 and Podoplanin showed the elimination of lymphatics 30 days after injection, and significantly lower number of lymphatics even after 75 days (Figure 15).

Functional analysis was performed by the injection of 70 kDa Rhodamine-dextran into the hind limbs of previously PBS (phosphate buffered saline) or Diphtheria Toxin treated animals. 30 and 75 days after injection mean fluorescent intensity of the popliteal lymph nodes showed decreased showing decreased uptake of the tracer molecule in the Diphtheria Toxin treated hind limb, while the signal was detectable in the popliteal region of the PBS treated animals. Quantification of the data showed significant reduction of the popliteal fluorescent signal in Diphtheria Toxin injected animals compared to PBS injected ones 30 and 75 days after the treatment (Figure 16).

Taken together, the presented results indicated that experimental secondary lymphedema was effectively developed in the *Flt4-CreER^{T2}; iDTR$^{fl/fl}$* mouse model.

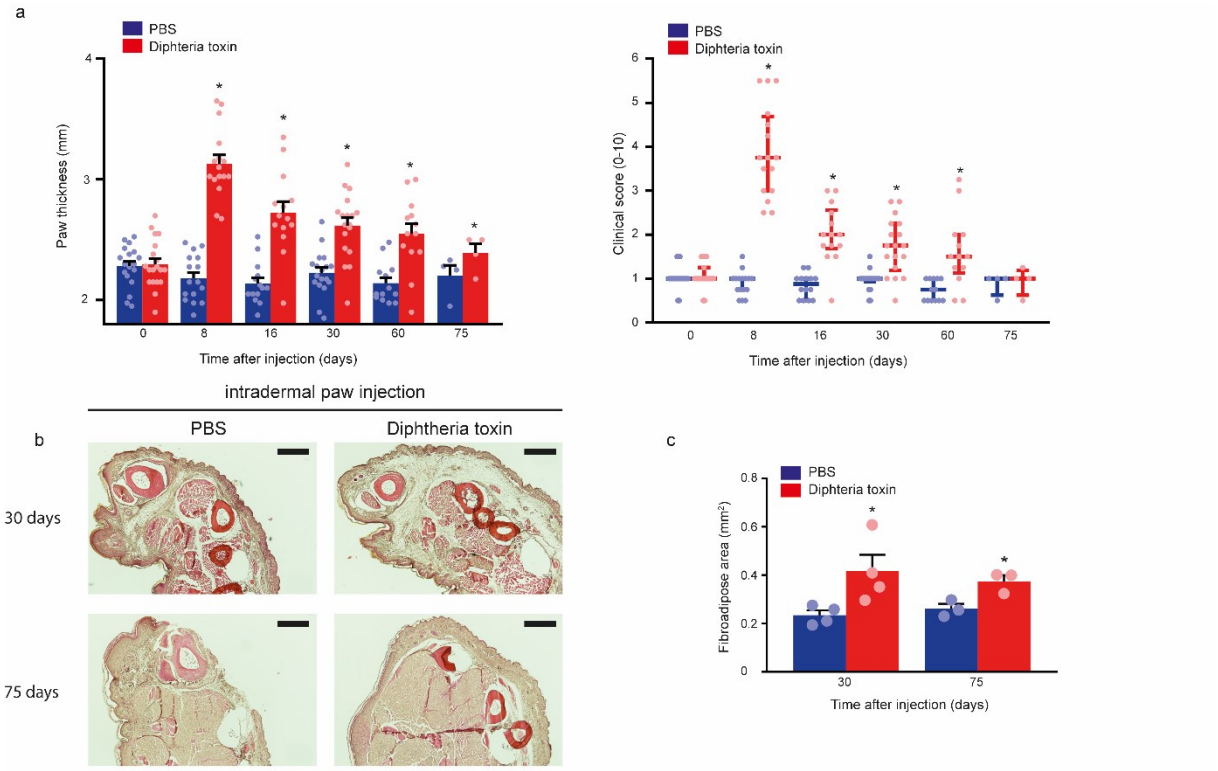

Figure 14 Diphtheria Toxin Induces Experimental Secondary Lymphedema Development in *Flt4-CreER^{T2}; iDTR$^{fl/fl}$* Mice. "**(a)** Monitoring paw thickness and paw clinical score in tamoxifen-treated *Flt4-CreER^{T2}; iDTR$^{fl/fl}$* mice after treatment with PBS or Diphtheria toxin. Quantitative data are represented as mean and SEM for paw thickness and median and IQR (interquartile range) for clinical score (two-tailed, paired T-test for paw thickness $P = 4.21*10^{-12}$ on day 8 for 16 mice, $P = 5.05*10^{-6}$ on day 16 for 14 mice, $P = 1.62*10^{-5}$ on day 30 for 18 mice, $P = 0.0008$ on day 60 for 13 mice, and $P = 0.0112$ on day 75 for 4 mice. Two-tailed Wilcoxon signed-rank test for clinical score $P = 3.05*10^{-5}$ on day 8 for 16 mice, $P = 0.0002$ on day 16 for 14 mice, $P = 6.10*10^{-5}$ on day 30 for 18 mice, $P = 0.0020$ on day 60 for 13 mice, and $P > 0.9999$ on day 75 for 4 mice). **(b)** Hematoxylin and Eosin staining of the paws of *Flt4-CreER^{T2}; iDTR$^{fl/fl}$* tamoxifen-treated mice 30 and 75 days after treatment with PBS or Diphtheria toxin. Representative images are shown of 5 mouse paws per group (bars, 200 µm). **(c)** Paw fibroadipose area of tamoxifen-treated *Flt4-CreER^{T2}; iDTR$^{fl/fl}$* mice 30 and 75 days after intradermal paw injection with PBS or Diphtheria toxin. Quantitative data are represented as mean and SEM (two-tailed, paired T-test, $P = 0.0469$ on day 30 for 4 mice and $P = 0.0172$ on day 75 for 3 mice). Asterisks indicate $P < 0.05$ compared with control." [I]

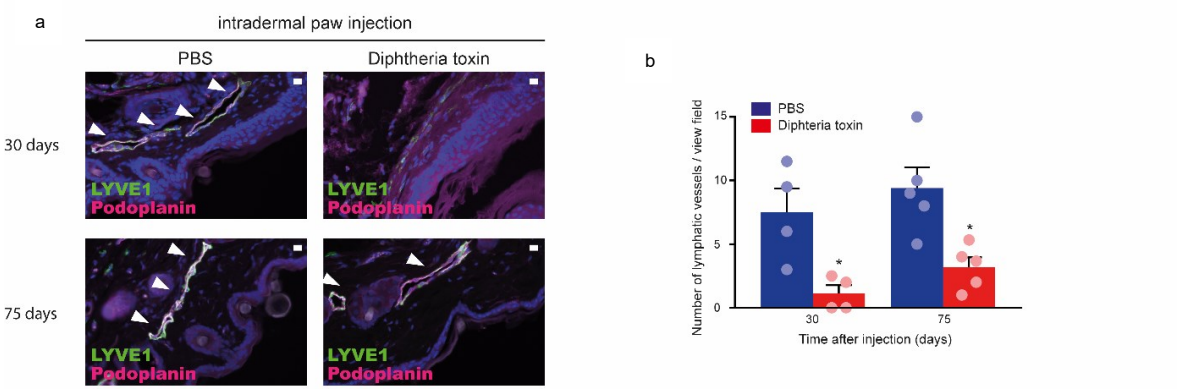

Figure 15 Diphtheria Toxin Eliminates Lymphatics *Flt4-CreER^{T2}; iDTR$^{fl/fl}$* Mice. "**(a)** Representative images of anti-LYVE1 and anti-Podoplanin immunostaining of the paws of *Flt4-CreERT2; iDTR$^{fl/fl}$* tamoxifen-treated mice 30 and 75 days after treatment with PBS or Diphtheria toxin. Representative images are shown of 4–5 mouse paws in each group (bars, 50 µm). Arrows indicate LYVE1 and Podoplanin double positive lymphatic vessels. **(b)** Number of lymphatic vessels of tamoxifen-treated *Flt4-CreERT2; iDTR$^{fl/fl}$* mice 30 and 75 days after intradermal paw injection with PBS or Diphtheria toxin. Quantitative data are represented as mean and SEM from 4–5 mouse paws in each group (two-tailed, paired T-test, P = 0.0319 after 30 days for 4 mice and P = 0.0434 after 75 days for 5 mice). Asterisks indicate P < 0.05 compared with control. All cell nuclei are labeled with DAPI (blue) in paraffin-embedded tissues." [I]

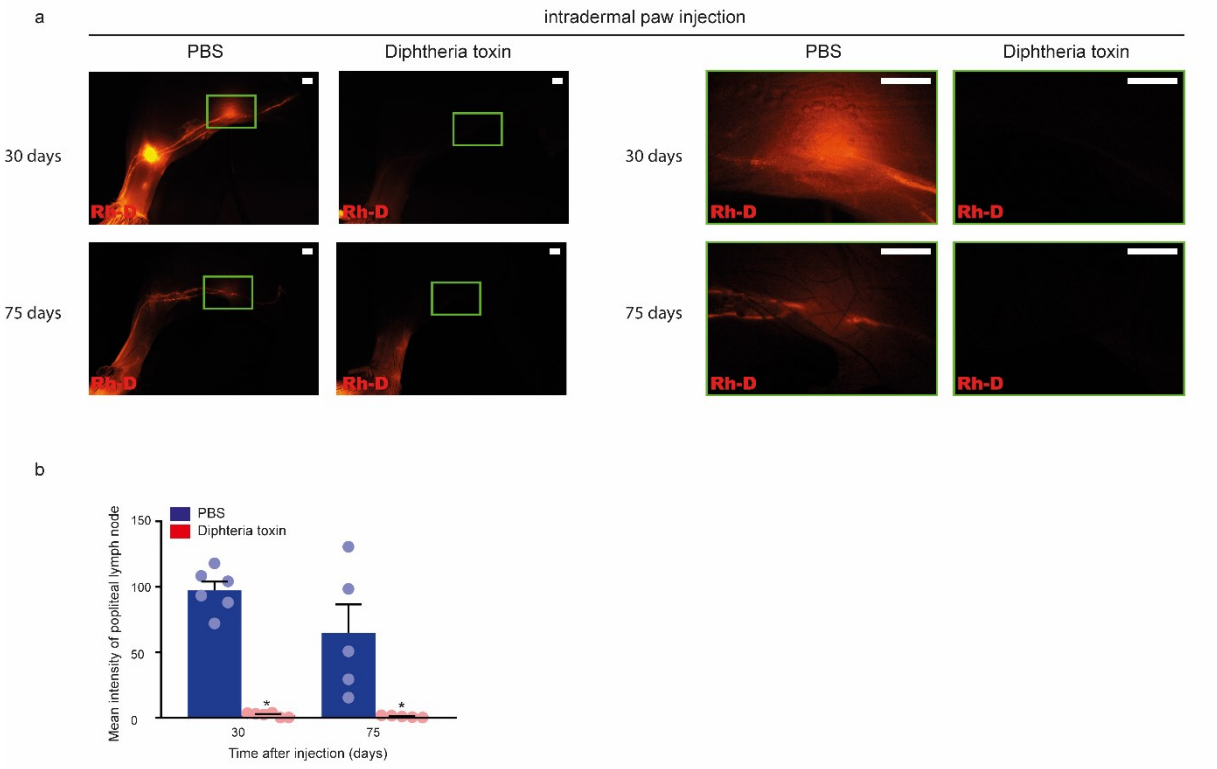

Figure 16 Administration of Diphtheria Toxin into the Paws of Tamoxifen-Treated *Flt4-CreER^{T2}; iDTR$^{fl/fl}$* Animals Reduces Lymphatic Function as the Result of Secondary Lymphedema Development. "**(a)** Monitoring active lymphatic function in the contralateral hind limbs of the same tamoxifen-treated *Flt4-CreER^{T2}; iDTR$^{fl/fl}$* mouse 30 or 75 days after intradermal injection of PBS into one paw and Diphtheria toxin into another paw. 70 kDa Rh-D was injected into the paws and the transport of the molecule was monitored by fluorescent microscopy 90 min post Rh-D administration. Representative images are shown of 5–6 mouse hind limbs in each group. (bars, 1000 µm). Green rectangles show the magnified area which represent the area of popliteal lymph nodes. **(b)** Fluorescent intensity of popliteal lymph node of tamoxifen-treated *Flt4-CreER^{T2}; iDTR$^{fl/fl}$* mice 30 and 75 days after intradermal paw injection with PBS or Diphtheria toxin. 70 kDa Rh-D was injected into the paws and the transport of the molecule was monitored by fluorescent microscopy 90 min post Rh-D administration. Quantitative data are represented as mean and SEM in 5–6 popliteal lymph nodes in each group (two-tailed, paired T-test, $P = 4.51*10^{-5}$ after 30 days for 6 mice and $P = 0.0421$ after 75 days for 5 mice). Asterisks indicate $P < 0.05$ compared with control." [I]

3.7. VEGFC mRNA-LNP Reverses Lymphedema in an in Vivo Genetic Mouse Model

After the development and setup of the genetic secondary lymphedema mouse model, 1 µg of Poly(C) or VEGFC mRNA-LNP was injected 8 days after the first Diphtheria Toxin injection of the paws. Paw thickness and clinical score of the lymphedema were significantly reduced 30, 60 and 75 days after the first Diphtheria Toxin injection (Figure 17a).

Histological analysis showed that fibroadipose area, which is a sign of secondary lymphedema, was also reduced after VEGFC mRNA-LNP injection compared to control (Figure 17b, c). Immunohistochemistry against LYVE1 and Podoplanin lymphatic vessel markers showed significant increase in the number of lymphatic vessels (Figure 18).

Functional analysis was performed by the injection of 70 kDa fluorescently labeled Rhodamine-dextran into the previously Poly(C) or VEGFC mRNA-LNP injected paws, that were previously treated with Diphtheria Toxin. Mean fluorescent intensity of the popliteal lymph nodes increased showing increased uptake of the tracer molecule in the VEGFC mRNA-LNP treated hind limb, while only minimal signal could be detected in the popliteal region of the Poly(C) mRNA-LNP treated animals. Quantification of the data showed significant growth of the popliteal fluorescent signal in VEGFC mRNA-LNP treated animals compared to Poly(C) RNA LNP injected ones (Figure 19).

In summary, VEGFC mRNA-LNP is an effective rescue therapy after Diphtheria Toxin injection in the genetic secondary lymphedema mouse model. Therefore, these findings demonstrate a proof of concept for VEGFC mRNA-LNP being an excellent tool to induce functional lymphatic vessel growth, and to reverse experimental lymphedema.

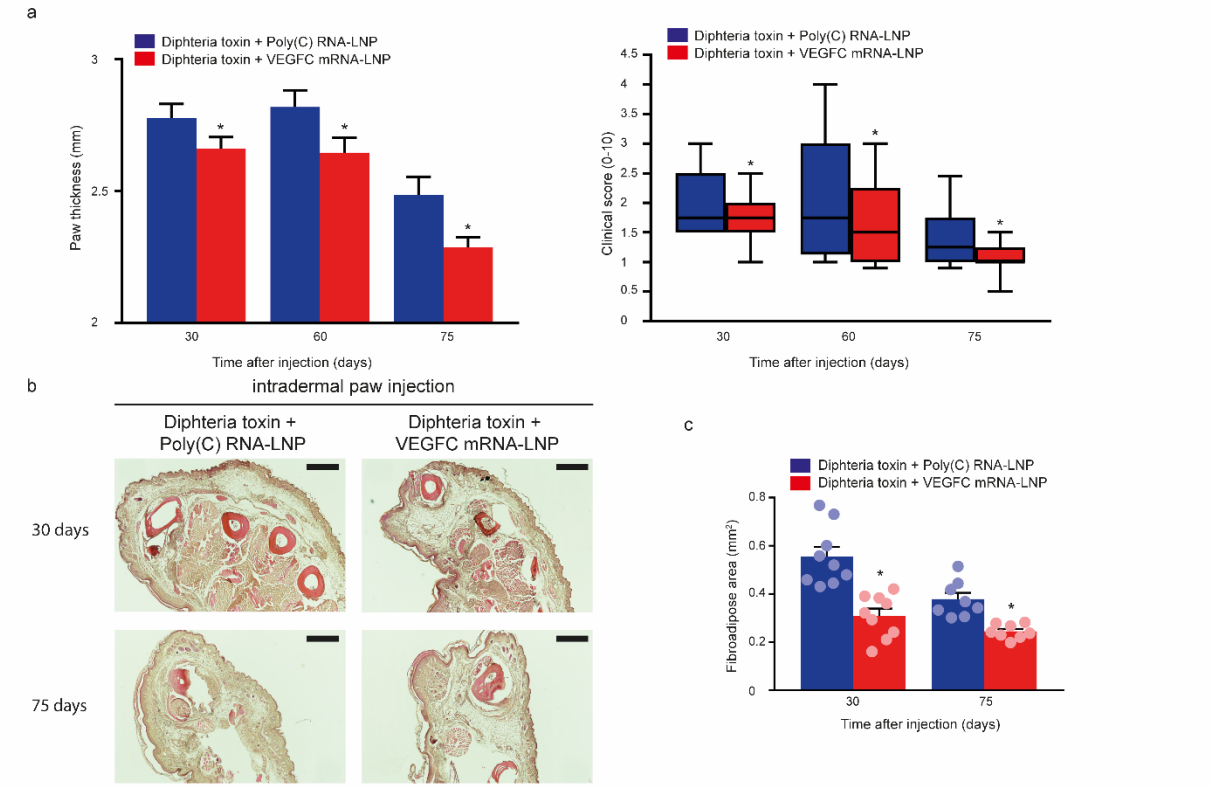

Figure 17 VEGFC mRNA-LNP Treatment Reverses Experimental Lymphedema. "**(a)** Monitoring paw thickness and clinical score in Diphtheria toxin and tamoxifen-treated *Flt4-CreER^{T2}; iDTR$^{fl/fl}$* mice intradermally injected with 1 µg of Poly(C) or VEGFC mRNA-LNPs. Data are represented as mean and SEM for paw thickness and box shows median and 25th to 75th percentiles, and whiskers show 10th–90th percentiles for clinical score (two-tailed, paired T-test, for paw thickness P = 0.0090 on days 30 for 31 mice, P = 0.0053 on day 60 for 25 mice and P = 0.0082 on day 75 for 15 mice. Two-tailed Wilcoxon signed-rank test for clinical score P = 0.0050 on day 30 for 31 mice, P = 0.0278 on day 60 for 25 mice, and P = 0.0469 on day 75 for 15 mice). **(b)** Hematoxylin and Eosin histology of the paws of tamoxifen-treated *Flt4-CreER^{T2}; iDTR$^{fl/fl}$* mice 30 and 75 days after treatment with Diphtheria toxin and 1 µg of Poly(C) or Diphtheria toxin and 1 µg of VEGFC mRNA-LNPs intradermally. Poly(C) or VEGFC mRNA-LNPs were injected 8 days after Diphtheria toxin treatment. Representative images are shown of 5 mouse paws in each group (bars, 200 µm). **(c)** Paw fibroadipose area of tamoxifen-treated *Flt4-CreER^{T2}; iDTR$^{fl/fl}$* mice 30 and 75 days after treatment with Diphtheria toxin and 1 µg of Poly(C) or Diphtheria toxin and 1 µg of VEGFC mRNA-LNPs. Poly(C) or VEGFC mRNA-LNPs were injected 8 days after Diphtheria toxin treatment. Quantitative data are represented as mean and SEM (two-tailed, paired T-test, P = 0.0001 on day 30 for 9 mice

and P = 0.0047 on day 75 for 8 mice). Asterisks indicate P < 0.05 compared with control." [I]

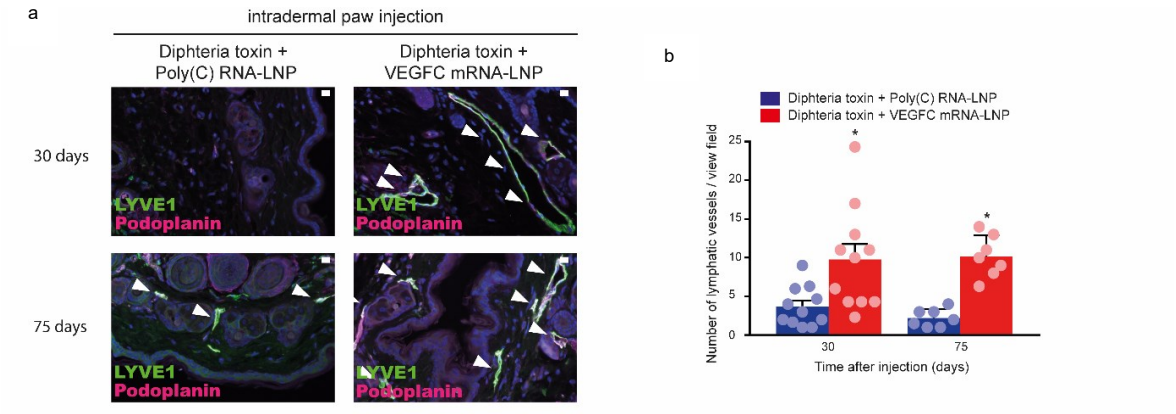

Figure 18 VEGFC mRNA-LNP Treatment Regrew Lymphatics Effectively in Secondary Lymphedema Mouse Model. "**(a)** Anti-LYVE1, anti-Podoplanin immunofluorescent histology of the paws of tamoxifen-treated Flt4-CreER^{T2}; iDTR$^{fl/fl}$ mice 30 and 75 days after treatment with Diphtheria toxin and 1 µg of Poly(C) or Diphtheria toxin and 1 µg of VEGFC mRNA-LNPs. Poly(C) or VEGFC mRNA-LNPs were injected 8 days after Diphtheria toxin treatment. Representative images are shown of 5 mouse paws in each group (bars, 50 µm). Arrows indicate LYVE1 and Podoplanin double positive lymphatic vessels. **(b)** Number of lymphatic vessels of tamoxifen-treated *Flt4-CreER^{T2}; iDTR$^{fl/fl}$* mice 30 and 75 days after the paw treatment with Diphtheria toxin and 1 µg of Poly(C) or Diphtheria toxin and 1 µg of VEGFC mRNA-LNPs. Poly(C) or VEGFC mRNA-LNPs were injected 8 days after Diphtheria toxin treatment. Quantitative data are represented as mean and SEM in 7–11 mouse paws in each group (two-tailed, paired T-test, P = 0.0024 after 30 days for 11 mice and P = 0.0008 after 75 days for 7 mice). Asterisks indicate P < 0.05 compared with control. All cell nuclei are labeled with DAPI (blue) in paraffin-embedded tissues." [I]

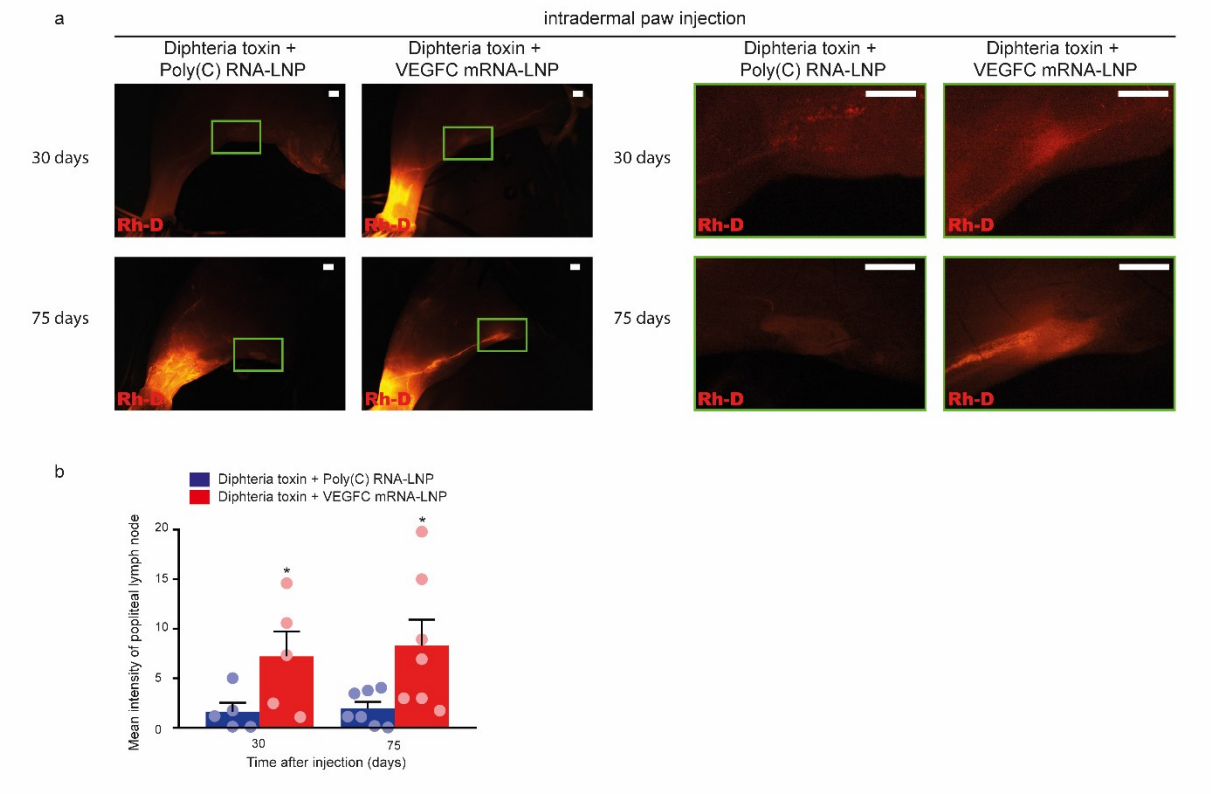

Figure 19 VEGFC mRNA-LNP Treatment Restores Lymphatic Function in Experimental Lymphedema. "**(a)** Monitoring active lymphatic function in the contralateral hind limbs of the same tamoxifen-treated *Flt4-CreER^{T2}; iDTR$^{fl/fl}$* mouse 30 or 75 days after the injection of Diphtheria toxin and 1 µg of Poly(C) into one paw and Diphtheria toxin and 1 µg of VEGFC mRNA-LNPs into the contralateral paw. Poly(C) or VEGFC mRNA-LNPs were injected 8 days after Diphtheria toxin treatment. 70 kDa Rh-D was injected into the paws and the transport of the molecule was monitored by fluorescent microscopy 90 min post Rh-D administration. Representative images are shown of 5-7 mouse hind limbs in each group (bars, 1000 µm). Green rectangles show the magnified area which represent the area of popliteal lymph nodes. **(b)** Fluorescent intensity of popliteal lymph nodes of tamoxifen-treated *Flt4-CreER^{T2}; iDTR$^{fl/fl}$* mice 30 and 75 days after the injection of Diphtheria toxin and 1 µg of Poly(C) into one paw and Diphtheria toxin and 1 µg of VEGFC mRNA-LNPs into another paw. Poly(C) or VEGFC mRNA-LNPs were injected 8 days after Diphtheria toxin treatment. 70 kDa Rh-D was injected into the paws and the transport of the molecule was monitored by fluorescent microscopy 90 min post Rh-D administration. Quantitative data are represented as mean and SEM in 5–7 popliteal lymph nodes in each group (two-tailed, paired T-test, $P = 0.0425$ after 30 days for 5 mice and $P = 0.0373$ after 75 days for 7 mice). Asterisks indicate $P < 0.05$ compared with control." [I]

3.8. Newborn Clp1$^{K/K}$ Mice Are Cyanotic, Show Signs of Respiratory Failure, and Die Shortly After Birth

In the next series of experiments, we set up and examined the *Clp1*$^{K/K}$ transgenic mouse model to assess organ-specific lymphatic function in the developing lung.

First, we set up timed mating between heterozygous adult animals. Embryos were removed from their mother by performing cesarean section at E19.5 (embryonic day 19.5). The genotype for the *Clp1* gene was verified with allele specific polymerase chain reaction (PCR).

Then, we examined newborn *Clp1*$^{K/K}$ mice and their viability and ability to breath. We found that *Clp1*$^{K/K}$ newborns were cyanotic and died shortly after birth, while control animals survived the intervention (Figure 20).

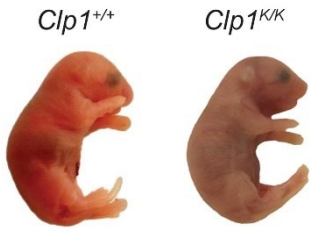

Figure 20 *Clp1*$^{K/K}$ Newborns Develop Respiratory Failure, and Die After Birth. Appearance of newborn *Clp1*$^{+/+}$ and *Clp1*$^{K/K}$ littermates on a C57BL/6 genetic background. Representative images are shown of 15–19 embryos from six litters. [II]

3.9. $Clp1^{K/K}$ Late Gestation Embryo Performs Less FBMs

Fetal breathing movements develop in late gestation mouse embryos and can be observed with ultrasound although this technique has great limitations [58].

We performed cesarean section in anesthetized mice, and removed the uterus from the abdomen. Then, we observed the movements of the embryos with ultrasound, and measured the number of fetal breathing movements during a 2-minute-long period.

We found that E18.5 $Clp1^{+/+}$ and $Clp1^{K/+}$ control embryos performed 2.67 ± 1.12 FBMs in 2 minutes (mean and SEM) (five out of six control embryos performed FBMs), while no FBM was found in one $Clp1^{K/K}$ embryo with normal heart activity. The diaphragm of the control animals slid, while the one of the $Clp1^{K/K}$ embryos did not move (Figures 21, 22). There were 2 other litters at E18.5 which (control and non-control embryos overall) showed no FBM activity. Therefore, these animals were excluded from the study.

Collectively, our data indicate that $Clp1^{K/K}$ is a great genetic mouse model to study the role of FBMs and its physiologic effects on lymphatic vessels.

Later in our article, we showed that late gestation $Clp1^{K/K}$ embryos display reduced prenatal lymphatic function, and impaired lung expansion represented as thickened alveolar septae and reduced alveolar area. These findings suggest a possible mechanism that FBMs, similarly to breathing movements after birth, stimulate prenatal lymphatic function in pulmonary collecting lymphatics lacking smooth muscle coverage to prepare the developing lung for inflation and gas exchange at birth. [II]

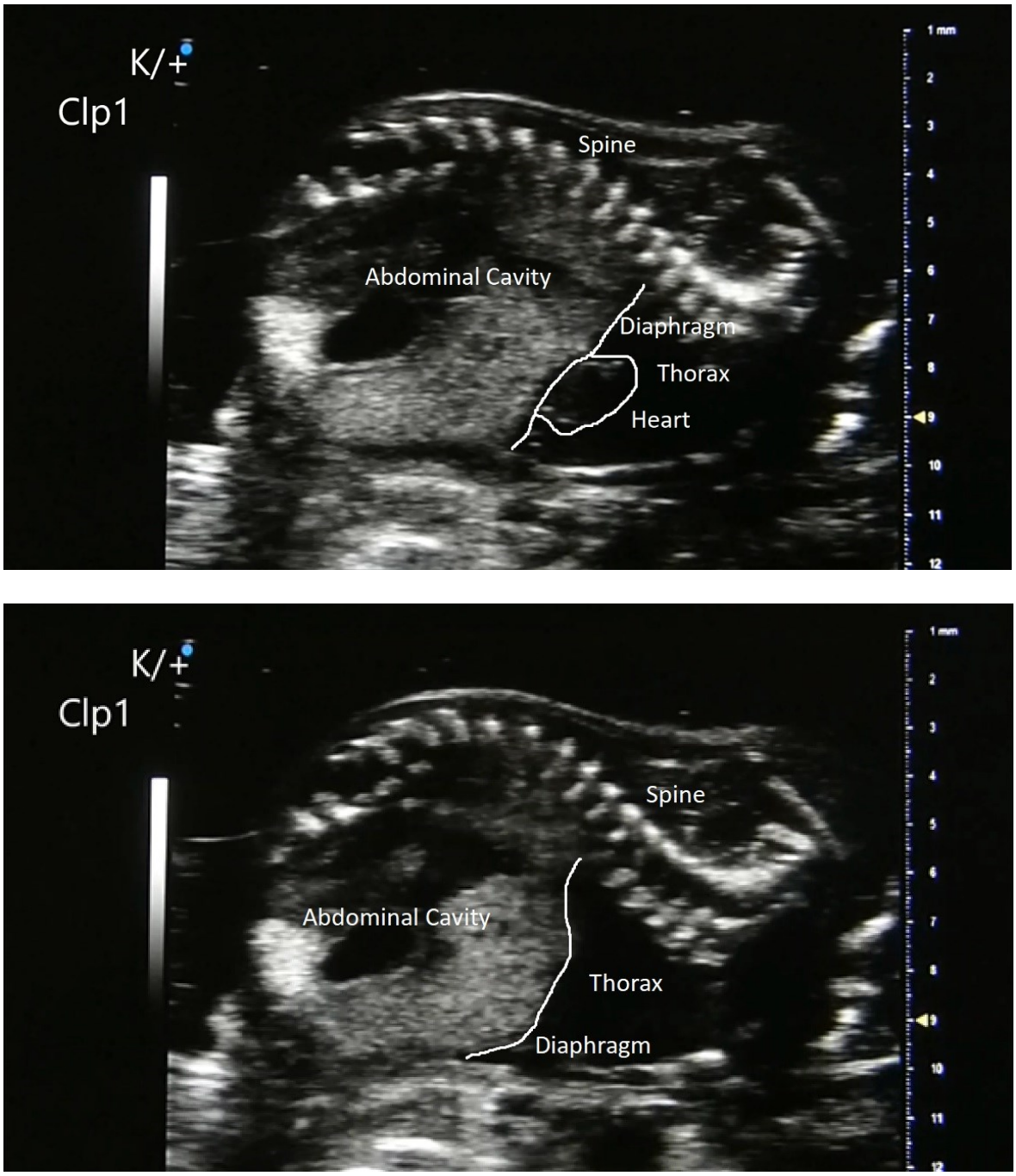

Figure 21 Representative Ultrasound Images of Late Gestation *Clp1*$^{K/+}$ Control Embryo at E18.5. *Clp1*$^{K/+}$ embryos performed FBMs. FBMs can be seen as the movement of the diaphragm. Images were taken by a Visualsonics Vevo 3100 imaging system, MX400 linear transducer with 30 MHz, 55 fps, B mode. [II]

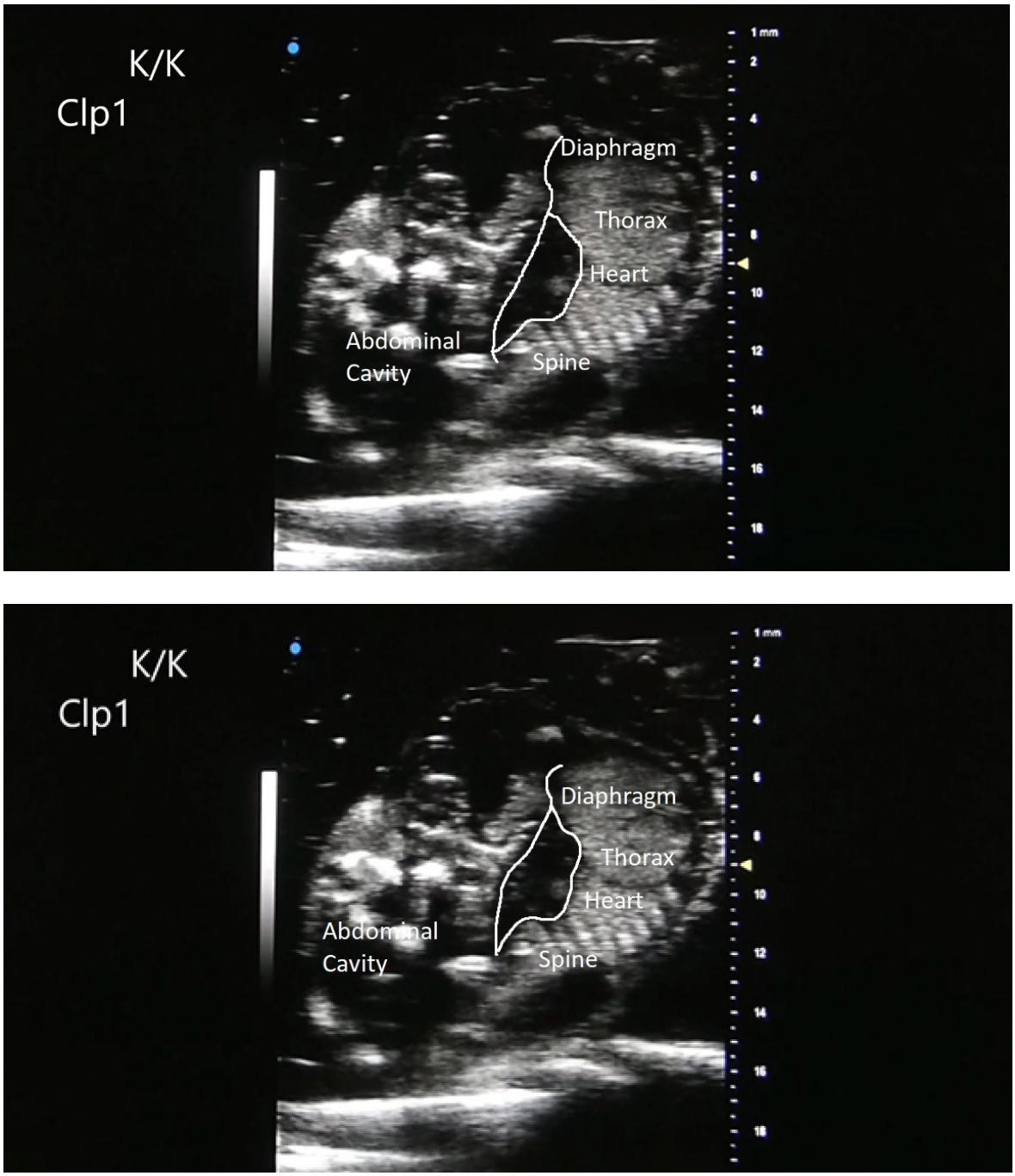

Figure 22 Representative Ultrasound Images of Late Gestation *Clp1*$^{K/K}$ Embryo at E18.5. *Clp1*$^{K/K}$ embryo did not perform FBMs. The diaphragm did not move. Images were taken by a Visualsonics Vevo 3100 imaging system, MX400 linear transducer with 30 MHz, 55 fps, B mode. [II]

4. Discussion

Recently, more and more different functions of the lymphatics were discovered. We realized that lymphatic anatomy and function vary in different organs. Therefore, it is important to study the organ-specific physiologic and pathophysiologic role of lymphatics in different organs and different diseases. First, we studied stimulated lymphatic function in the skin in secondary lymphedema. Second, we set up a model to examine absent fetal breathing movements and its effects on lymphatic function in the developing lung of newborn mice.

The nucleoside-modified mRNA-LNP platform is a new therapeutic approach which was used in recent years for vaccine development, protein therapy, and gene editing in many studies. This approach showed to be safe and effective. Moderna and Pfizer/BioNTech developed vaccines based upon this system during the COVID-19 pandemic, and these vaccines demonstrated the safety and efficacy of the platform [77, 87-90, 105-107].

In our study, we showed that nucleoside modified VEGFC mRNA-LNP induces VEGFC protein expression *in vivo* and lymphatic vessel growth effectively in various organs in mice. The lymphatic vessel growing effect lasted for 60 days. The newly formed lymphatic vessels had typical morphology and demonstrated normal lymphatic function. In previous studies, viral vector-based VEGFC delivery resulted in lymphatic endothelial cell proliferation in some cases, but these cells were unable to form functional lymphatic vessels [22, 23]. After setting up a genetic lymphedema mouse model, we also demonstrated that only a single dose of VEGFC mRNA-LNP can effectively stimulate lymphatic growth and reverses lymphedema. This effect was present even 75 days after the treatment.

This study reports the first time using the mRNA-LNP platform to induce lymphatic vessel growth and examine its effects on lymphedema. Two other methods were used for VEGFC protein delivery before: direct injection of recombinant VEGFC protein, and expression of VEGFC *in vivo* via virus-vector delivery [7, 11, 22, 61-73]. The mRNA-LNP platform has several advantages over these two systems such as, simple production, lack of integration into the host genome, no anti-vector immunity, highly controllable administration by dosage and localization, long lasting protein production, and the lack of strong inflammation.

Our experiments showed that VEGFC protein expression and also lymphatic growth occurred only at the injection site, and there was no detectable lymphatic growth in other organs. These results indicate that VEGFC mRNA-LNP had only local effect.

Another possible side effect could have been the induction of blood vessel proliferation. Previous studies showed that VEGFC protein induces lymphatic vessel growth only, but VEGFD induces both lymphatic and blood vessel proliferation [104, 108]. Our results showed no significant blood vessel growth.

Previous studies showed that VEGFC is a chemoattractant for monocytes and macrophages [109, 110]. We found no significant increase in the number of immune cells when injected with VEGFC mRNA-LNP compared to control.

To investigate the effects of VEGFC mRNA-LNP on lymphedema, we rigorously tested a Diphtheria-toxin inducible genetic secondary lymphedema mouse model. We examined changes in paw thickness, clinical score of the disease, fibroadipose area, and lymphatic function. First, we set up and examined the *FLT4-CreER^{T2}; iDTR$^{fl/fl}$* secondary lymphedema mouse model. In this model lymphatic vessels were deleted, lymphedema developed and lasted up to 75 days after Diphtheria-toxin injection. Increased fibroadipose area was seen and we detected dramatically reduced lymphatic drainage to the regional lymph node in the Diphtheria-toxin injected limbs. Lymphedema development and lymphatic vessel deletion occurred only on the injection site and no systemic effect or obvious side effect was seen. Our findings were similar to the previous studies of Gardenier et al. In their series of experiments, lymphedema was developed after Diphtheria Toxin injection, which peaked at 7 days after injection. They found complete ablation of lymphatic vessels one week after Diphtheria Toxin injection at the injection site. Disrupted lymphatic function was also assessed by this research group [47]. These findings are all in accordance with our results.

A single dose administration of 1 µg VEGFC mRNA-LNP into limbs, in which previously lymphedema was induced, resulted in paw thickness, clinical score, and fibroadipose area reduction. New lymphatic vessels developed after the injection. Importantly, VEGFC mRNA-LNP treatment not only resulted in lymphatic vessel formation but the lymphatic function was also restored. This functioning lymphatic network was able to transport the macromolecules from the paws to the popliteal lymph nodes 30 and 75 days after disease induction.

These findings show, that the VEGFC mRNA-LNP platform can be a therapeutic agent for patients suffering from lymphedema. A viral vector VEGFC delivery platform (Lymfactin) is currently studied in clinical trial (Phase II, NCT03658967) in the treatment of secondary lymphedema [68, 111]. Adenovirus based systems have known side effects, including unspecific immune responses and host genome integration. The mRNA-LNP platform might be a safer alternative method for protein therapies, than viral vector delivery methods in the future. Although, our results are promising and we saw no obvious adverse effects, further studies are needed in the future, such as large animal studies before clinical application.

In our other set of experiments, we examined fetal breathing movements in a *Clp1*$^{K/K}$ embryo and breathing in newborns right after birth. *Clp1*$^{K/K}$ CLP1 kinase-dead mice were used which lose the innervation of skeletal muscle and therefore are paralyzed from E16.5 gestational age [102].

We found that *Clp1*$^{K/K}$ newborns were cyanotic after birth and died shortly. This occurred because of no effective respiratory muscle movements, so these newborns died in respiratory failure.

Lately, Niblock et al. showed that FBMs occur not only in large animals, but also in mice which was previously not noticeable, most likely because of anesthesia [58, 112]. The authors themselves affirmed that examination of pregnant mice with ultrasound without anesthesia is very challenging and has several difficulties. First, the pregnant female has to be still during the whole process, but anesthesia itself affects the FBMs. Then, thermoregulation of the female has to be solved. Another problem is that embryos – unlike newborns – do not regularly breathe, so the examiner has two opportunities to capture and examine FBMs. They either examine the embryo for a long time, which is time consuming, or stimulate FBMs and capture them at the exact moment.

Another challenge is that the *Clp1*$^{K/K}$ homozygous mutation is lethal. Thus, the breeding of this genotype cannot be achieved with homozygous parents. Mice have numerous embryos in a single litter, therefore the distinction between embryos is extremely difficult, while the uterus is inside the abdomen of the mother. Due to the previously mentioned challenge, the genotype of the embryos must be verified by PCR. Therefore, a section on the abdominal skin of the mother was performed followed by the externalization of the uterus. That way, tail samples could be collected from the exact embryos for PCR and the

captured recording could be paired with the samples, after the ultrasound examination was performed on all embryos. However, this method presented another challenge, as the ultrasound videos had to be recorded rapidly to prevent the effect of cooling on the FBMs. Despite the difficulties we found that the *Clp1*$^{K/K}$ embryo performed no FBMs in the examined period of time, while we detected FBMs when examined *Clp1*$^{+/+}$ or *Clp1*$^{K/+}$ control embryos.

These findings indicate that *Clp1*$^{K/K}$ embryos are great genetic models for examining the roles of FBMs and its effects on lymphatic anatomy and function. It has great potential to research the role of FBMs on the lymphatic vessels in the developing lung. Later in our article we showed that lymphatic anatomy is altered and lymphatic function is decreased in *Clp1*$^{K/K}$ embryos. We are willing to stimulate FBMs of late gestation mouse embryos, and examine organ specific lymphatic function in future studies.

5. Conclusions

- We described a novel application of the nucleoside-modified mRNA-LNP therapeutic platform as an effective protein delivery system to trigger lymphangiogenic VEGFC expression.

- We showed that the administration of a single low dose of VEGFC mRNA-LNPs induces durable, organ-specific lymphatic growth, and formation of fully functional new lymphatic vessels.

- We designed and evaluated a novel gain of function approach for identifying the organ-specific physiological and pathophysiological roles of the lymphatic system.

- We showed that the nucleoside-modified VEGFC mRNA-LNP platform is effective in reversing disease progression in an experimental lymphedema mouse model by inducing the formation of a functional lymphatic network.

- We showed that *Clp1*$^{K/K}$ transgenic newborn mice are cyanotic, cannot breathe effectively, and die shortly after birth due to respiratory failure.

- We developed and applied an ultrasound-based technique to detect fetal breathing movements during the late gestation period in mice despite numerous technical challenges. Our results indicate that *Clp1*$^{K/K}$ embryos might perform less fetal breathing movements compared to controls.

6. Summary

Novel roles of the lymphatic system were identified lately and made us realize that lymphatic vessels vary in an organ specific manner. In this study, we wanted to identify the organ specific functions of the lymphatics in the skin in lymphedema and in the lungs in respiratory adaptation of the newborn. Lack or dysfunction of the lymphatics in the skin leads to secondary lymphedema. There is no definitive treatment for lymphedema, only symptomatic relief. Lately, new organ specific functions of the lymphatics were identified in the developing lung. Newborn mice look cyanotic, die shortly after birth in respiratory failure in mouse models with disturbed lymphangiogenic factors.

To examine the organ-specific role of lymphatics in the skin, we wanted to develop an mRNA-LNP based tool to stimulate lymphatic function and used it in a secondary lymphedema mouse model in the skin. To study the role of organ-specific function of lymphatic vessels in the developing lung, we aimed to test whether the absence of late gestation FBMs have an impact on respiratory failure of the newborn and on lymphatic morphology and function in the lung.

We developed and produced nucleoside-modified murine VEGFC mRNA encapsulated in LNPs to stimulate lymphatic growth and function. We showed that VEGFC mRNA-LNPs induced organ-specific lymphatic growth without obvious adverse effects. Importantly, VEGFC mRNA-LNP treatment reversed experimental lymphedema in a secondary lymphedema mouse model. In the next series of experiments, we showed that *Clp1*$^{K/K}$ transgenic mice cannot survive after birth and one showed no fetal breathing movements *in utero*. Later, we demonstrated that the lack of FBMs results in reduced lymphatic function. (Data will be shown in another PhD thesis.)

Collectively, we revealed new mechanisms and understand now better organ-specific functions of the lymphatic system after we described two different mouse models in lymphedema in the skin and in respiratory failure of the newborn in mice. We presented that nucleoside-modified mRNA-LNP platform stimulates lymphatic growth and function. We found that stimulation of lymphatic function can be advantageous in secondary lymphedema. Furthermore, we developed an excellent model to examine the role of FBMs in lung development and lymphatic function.

In general, these findings indicate that stimulation of the lymphatic function in various organs can help us better understand different functions of the lymphatic system and develop new therapeutic approaches in the future.

7. References

1. Schulte-Merker, S., A. Sabine, and T.V. Petrova, *Lymphatic vascular morphogenesis in development, physiology, and disease.* J. Cell Biol., 2011. **193**(4): p. 607-618.

2. Oliver, G., J. Kipnis, G.J. Randolph, and N.L. Harvey, *The Lymphatic Vasculature in the 21st Century: Novel Functional Roles in Homeostasis and Disease.* Cell, 2020. **182**(2): p. 270-296.

3. Bálint, L. and Z. Jakus, *Mechanosensation and Mechanotransduction by Lymphatic Endothelial Cells Act as Important Regulators of Lymphatic Development and Function.* Int. J. Mol. Sci., 2021. **22**(8): p. 1-18.

4. Machnik, A., W. Neuhofer, J. Jantsch, A. Dahlmann, T. Tammela, K. Machura, J.K. Park, F.X. Beck, D.N. Müller, W. Derer, J. Goss, A. Ziomber, P. Dietsch, H. Wagner, N. van Rooijen, A. Kurtz, K.F. Hilgers, K. Alitalo, K.U. Eckardt, F.C. Luft, D. Kerjaschki, and J. Titze, *Macrophages regulate salt-dependent volume and blood pressure by a vascular endothelial growth factor-C-dependent buffering mechanism.* Nat. Med., 2009. **15**(5): p. 545-552.

5. Harvey, N.L., R.S. Srinivasan, M.E. Dillard, N.C. Johnson, M.H. Witte, K. Boyd, M.W. Sleeman, and G. Oliver, *Lymphatic vascular defects promoted by Prox1 haploinsufficiency cause adult-onset obesity.* Nat. Genet., 2005. **37**(10): p. 1072-1081.

6. Klotz, L., S. Norman, J.M. Vieira, M. Masters, M. Rohling, K.N. Dubé, S. Bollini, F. Matsuzaki, C.A. Carr, and P.R. Riley, *Cardiac lymphatics are heterogeneous in origin and respond to injury.* Nature, 2015. **522**(7554): p. 62-67.

7. Henri, O., C. Pouehe, M. Houssari, L. Galas, L. Nicol, F. Edwards-Lévy, J.P. Henry, A. Dumesnil, I. Boukhalfa, S. Banquet, D. Schapman, C. Thuillez, V. Richard, P. Mulder, and E. Brakenhielm, *Selective Stimulation of Cardiac Lymphangiogenesis Reduces Myocardial Edema and Fibrosis Leading to Improved Cardiac Function Following Myocardial Infarction.* Circulation, 2016. **133**(15): p. 1484-1497; discussion 1497.

8. Martel, C., W. Li, B. Fulp, A.M. Platt, E.L. Gautier, M. Westerterp, R. Bittman, A.R. Tall, S.H. Chen, M.J. Thomas, D. Kreisel, M.A. Swartz, M.G. Sorci-Thomas, and

G.J. Randolph, *Lymphatic vasculature mediates macrophage reverse cholesterol transport in mice.* J. Clin. Invest., 2013. **123**(4): p. 1571-1579.

9. Aspelund, A., S. Antila, S.T. Proulx, T.V. Karlsen, S. Karaman, M. Detmar, H. Wiig, and K. Alitalo, *A dural lymphatic vascular system that drains brain interstitial fluid and macromolecules.* The Journal of experimental medicine, 2015. **212**(7): p. 991-999.

10. Louveau, A., J. Herz, M.N. Alme, A.F. Salvador, M.Q. Dong, K.E. Viar, S.G. Herod, J. Knopp, J.C. Setliff, A.L. Lupi, S. Da Mesquita, E.L. Frost, A. Gaultier, T.H. Harris, R. Cao, S. Hu, J.R. Lukens, I. Smirnov, C.C. Overall, G. Oliver, and J. Kipnis, *CNS lymphatic drainage and neuroinflammation are regulated by meningeal lymphatic vasculature.* Nat. Neurosci., 2018. **21**(10): p. 1380-1391.

11. Da Mesquita, S., A. Louveau, A. Vaccari, I. Smirnov, R.C. Cornelison, K.M. Kingsmore, C. Contarino, S. Onengut-Gumuscu, E. Farber, D. Raper, K.E. Viar, R.D. Powell, W. Baker, N. Dabhi, R. Bai, R. Cao, S. Hu, S.S. Rich, J.M. Munson, M.B. Lopes, C.C. Overall, S.T. Acton, and J. Kipnis, *Functional aspects of meningeal lymphatics in ageing and Alzheimer's disease.* Nature, 2018. **560**(7717): p. 185-191.

12. Jakus, Z., J.P. Gleghorn, D.R. Enis, A. Sen, S. Chia, X. Liu, D.R. Rawnsley, Y. Yang, P.R. Hess, Z. Zou, J. Yang, S.H. Guttentag, C.M. Nelson, and M.L. Kahn, *Lymphatic function is required prenatally for lung inflation at birth.* J. Exp. Med., 2014. **211**(5): p. 815-826.

13. Yang, Y., J.M. García-Verdugo, M. Soriano-Navarro, R.S. Srinivasan, J.P. Scallan, M.K. Singh, J.A. Epstein, and G. Oliver, *Lymphatic endothelial progenitors bud from the cardinal vein and intersomitic vessels in mammalian embryos.* Blood, 2012. **120**(11): p. 2340-2348.

14. Martinez-Corral, I., M.H. Ulvmar, L. Stanczuk, F. Tatin, K. Kizhatil, S.W. John, K. Alitalo, S. Ortega, and T. Makinen, *Nonvenous origin of dermal lymphatic vasculature.* Circ Res, 2015. **116**(10): p. 1649-1654.

15. Stanczuk, L., I. Martinez-Corral, M.H. Ulvmar, Y. Zhang, B. Laviña, M. Fruttiger, R.H. Adams, D. Saur, C. Betsholtz, S. Ortega, K. Alitalo, M. Graupera, and T. Mäkinen, *cKit Lineage Hemogenic Endothelium-Derived Cells Contribute to Mesenteric Lymphatic Vessels.* Cell Rep, 2015. **10**(10): p. 1708-1721.

16. Wigle, J.T., N. Harvey, M. Detmar, I. Lagutina, G. Grosveld, M.D. Gunn, D.G. Jackson, and G. Oliver, *An essential role for Prox1 in the induction of the lymphatic endothelial cell phenotype.* Embo j, 2002. **21**(7): p. 1505-1513.

17. González-Loyola, A. and T.V. Petrova, *Development and aging of the lymphatic vascular system.* Advanced Drug Delivery Reviews, 2021. **169**: p. 63-78.

18. Ma, W., H.J. Gil, X. Liu, L.P. Diebold, M.A. Morgan, M.J. Oxendine-Burns, P. Gao, N.S. Chandel, and G. Oliver, *Mitochondrial respiration controls the Prox1-Vegfr3 feedback loop during lymphatic endothelial cell fate specification and maintenance.* Sci Adv, 2021. **7**(18): p. 1-16.

19. Petrova, T.V., T. Mäkinen, T.P. Mäkelä, J. Saarela, I. Virtanen, R.E. Ferrell, D.N. Finegold, D. Kerjaschki, S. Ylä-Herttuala, and K. Alitalo, *Lymphatic endothelial reprogramming of vascular endothelial cells by the Prox-1 homeobox transcription factor.* Embo j, 2002. **21**(17): p. 4593-4599.

20. Veikkola, T., L. Jussila, T. Makinen, T. Karpanen, M. Jeltsch, T.V. Petrova, H. Kubo, G. Thurston, D.M. McDonald, M.G. Achen, S.A. Stacker, and K. Alitalo, *Signalling via vascular endothelial growth factor receptor-3 is sufficient for lymphangiogenesis in transgenic mice.* Embo j, 2001. **20**(6): p. 1223-1231.

21. Karkkainen, M.J., P. Haiko, K. Sainio, J. Partanen, J. Taipale, T.V. Petrova, M. Jeltsch, D.G. Jackson, M. Talikka, H. Rauvala, C. Betsholtz, and K. Alitalo, *Vascular endothelial growth factor C is required for sprouting of the first lymphatic vessels from embryonic veins.* Nat Immunol, 2004. **5**(1): p. 74-80.

22. Bui, H.M., D. Enis, M.R. Robciuc, H.J. Nurmi, J. Cohen, M. Chen, Y. Yang, V. Dhillon, K. Johnson, H. Zhang, R. Kirkpatrick, E. Traxler, A. Anisimov, K. Alitalo, and M.L. Kahn, *Proteolytic activation defines distinct lymphangiogenic mechanisms for VEGFC and VEGFD.* J. Clin. Invest., 2016. **126**(6): p. 2167-2180.

23. Jeltsch, M., S.K. Jha, D. Tvorogov, A. Anisimov, V.M. Leppanen, T. Holopainen, R. Kivela, S. Ortega, T. Karpanen, and K. Alitalo, *CCBE1 enhances lymphangiogenesis via A disintegrin and metalloprotease with thrombospondin motifs-3-mediated vascular endothelial growth factor-C activation.* Circulation, 2014. **129**(19): p. 1962-1971.

24. Le Guen, L., T. Karpanen, D. Schulte, N.C. Harris, K. Koltowska, G. Roukens, N.I. Bower, A. van Impel, S.A. Stacker, M.G. Achen, S. Schulte-Merker, and B.M.

Hogan, *Ccbe1 regulates Vegfc-mediated induction of Vegfr3 signaling during embryonic lymphangiogenesis.* Development, 2014. **141**(6): p. 1239-1249.

25. Alitalo, K., T. Tammela, and T.V. Petrova, *Lymphangiogenesis in development and human disease.* Nature, 2005. **438**(7070): p. 946-953.

26. Alders, M., B.M. Hogan, E. Gjini, F. Salehi, L. Al-Gazali, E.A. Hennekam, E.E. Holmberg, M.M. Mannens, M.F. Mulder, G.J. Offerhaus, T.E. Prescott, E.J. Schroor, J.B. Verheij, M. Witte, P.J. Zwijnenburg, M. Vikkula, S. Schulte-Merker, and R.C. Hennekam, *Mutations in CCBE1 cause generalized lymph vessel dysplasia in humans.* Nat. Genet., 2009. **41**(12): p. 1272-1274.

27. Grada, A.A. and T.J. Phillips, *Lymphedema: Pathophysiology and clinical manifestations.* J. Am. Acad. Dermatol., 2017. **77**(6): p. 1009-1020.

28. Rockson, S.G. and K.K. Rivera, *Estimating the population burden of lymphedema.* Ann N Y Acad Sci, 2008. **1131**: p. 147-154.

29. Földi, E., Földi, M. Lymphostatic disease. In: Földi, M., E. Földi, R. Strößenreuther, and S. Kubik (editors), *Földi's textbook of lymphology: for physicians and lymphedema therapists*. Elsevier Urban & Fischer, München, 2012: p. 193.

30. Schulze, H., M. Nacke, C. Gutenbrunner, and C. Hadamitzky, *Worldwide assessment of healthcare personnel dealing with lymphoedema.* Health Econ Rev, 2018. **8**(1): p. 10.

31. Smeltzer, D.M., G.B. Stickler, and A. Schirger, *Primary lymphedema in children and adolescents: a follow-up study and review.* Pediatrics, 1985. **76**(2): p. 206-218.

32. Morfoisse, F., A. Zamora, E. Marchaud, M. Nougue, L.H. Diallo, F. David, E. Roussel, E. Lacazette, A.C. Prats, F. Tatin, and B. Garmy-Susini, *Sex Hormones in Lymphedema.* Cancers (Basel), 2021. **13**(3).

33. Kurt, H., C.A. Arnold, J.E. Payne, M.J. Miller, R.J. Skoracki, and O.H. Iwenofu, *Massive localized lymphedema: a clinicopathologic study of 46 patients with an enrichment for multiplicity.* Mod Pathol, 2016. **29**(1): p. 75-82.

34. Gillespie, S.H., *Basic lymphoedema management: treatment and prevention of problems associated with lymphatic filariasis: Gerusa Dreyer, David Addiss, Patricia*

Dreyer, Joaquim Noroes. Hollis Publishing Company, 124 pages, paperback, ISBN 1-884186-17-3 (US$19.00). Int. J. Infect. Dis., 2004. **8**(5): p. 321.

35. Bull, R.H., J.N. Gane, J.E.C. Evans, A.E.A. Joseph, and P.S. Mortimer, *Abnormal lymph drainage in patients with chronic venous leg ulcers.* J. Am. Acad. Dermatol., 1993. **28**(4): p. 585-590.

36. Raju, S., J.B. Furrh, and P. Neglén, *Diagnosis and treatment of venous lymphedema.* J. Vasc. Surg., 2012. **55**(1): p. 141-149.

37. Butler, D.F., P.J. Malouf, R.C. Batz, and C.L. Stetson, *Acquired lymphedema of the hand due to herpes simplex virus type 2.* Arch. Dermatol., 1999. **135**(9): p. 1125-1126.

38. Asch, S., W.D. James, and L. Castelo-Soccio, *Massive localized lymphedema: An emerging dermatologic complication of obesity.* J. Am. Acad. Dermatol., 2008. **59**(5, Supplement): p. S109-S110.

39. Grada, A.A. and T.J. Phillips, *Lymphedema: Diagnostic workup and management.* J. Am. Acad. Dermatol., 2017. **77**(6): p. 995-1006.

40. *Radiation Inhibits Lymph Drainage in an Acquired Lymphedema Mouse Hindlimb Model.* Lymphat. Res. Biol., 2020. **18**(1): p. 16-21.

41. Yoon, Y.S., T. Murayama, E. Gravereaux, T. Tkebuchava, M. Silver, C. Curry, A. Wecker, R. Kirchmair, C.S. Hu, M. Kearney, A. Ashare, D.G. Jackson, H. Kubo, J.M. Isner, and D.W. Losordo, *VEGF-C gene therapy augments postnatal lymphangiogenesis and ameliorates secondary lymphedema.* J. Clin. Invest., 2003. **111**(5): p. 717-725.

42. Szuba, A., M. Skobe, M.J. Karkkainen, W.S. Shin, D.P. Beynet, N.B. Rockson, N. Dakhil, S. Spilman, M.L. Goris, H.W. Strauss, T. Quertermous, K. Alitalo, and S.G. Rockson, *Therapeutic lymphangiogenesis with human recombinant VEGF-C.* The FASEB Journal, 2002. **16**(14): p. 1985-1987.

43. Hagendoorn, J., T.P. Padera, S. Kashiwagi, N. Isaka, F. Noda, M.I. Lin, P.L. Huang, W.C. Sessa, D. Fukumura, and R.K. Jain, *Endothelial nitric oxide synthase regulates microlymphatic flow via collecting lymphatics.* Circ. Res., 2004. **95**(2): p. 204-209.

44. Weiler, M.J., M.T. Cribb, Z. Nepiyushchikh, T.S. Nelson, and J.B. Dixon, *A novel mouse tail lymphedema model for observing lymphatic pump failure during lymphedema development.* Sci. Rep., 2019. **9**(1): p. 10405.

45. Lee-Donaldson, L., M.H. Witte, M. Bernas, C.L. Witte, D. Way, and B. Stea, *Refinement of a rodent model of peripheral lymphedema.* Lymphology, 1999. **32**(3): p. 111-117.

46. Martinez-Corral, I., L. Stanczuk, M. Frye, M.H. Ulvmar, R. Dieguez-Hurtado, D. Olmeda, T. Makinen, and S. Ortega, *Vegfr3-CreER (T2) mouse, a new genetic tool for targeting the lymphatic system.* Angiogenesis, 2016. **19**(3): p. 433-445.

47. Gardenier, J.C., G.E. Hespe, R.P. Kataru, I.L. Savetsky, J.S. Torrisi, G.D. Nores, J.J. Dayan, D. Chang, J. Zampell, I. Martinez-Corral, S. Ortega, and B.J. Mehrara, *Diphtheria toxin-mediated ablation of lymphatic endothelial cells results in progressive lymphedema.* JCI Insight, 2016. **1**(15): p. e84095.

48. Avery, M.E. and J. Mead, *Surface properties in relation to atelectasis and hyaline membrane disease.* AMA J Dis Child, 1959. **97**(5, Part 1): p. 517-523.

49. Adams, F.H., T. Fujiwara, G. Emmanouilides, and A. Scudder, *Surface properties and lipids from lungs of infants with hyaline membrane disease.* The Journal of Pediatrics, 1965. **66**(2): p. 357-364.

50. Morgan, T.E., *Pulmonary surfactant.* N Engl J Med, 1971. **284**(21): p. 1185-1193.

51. Hintz, S.R., W.K. Poole, L.L. Wright, A.A. Fanaroff, D.E. Kendrick, A.R. Laptook, R. Goldberg, S. Duara, B.J. Stoll, and W. Oh, *Changes in mortality and morbidities among infants born at less than 25 weeks during the post-surfactant era.* Arch Dis Child Fetal Neonatal Ed, 2005. **90**(2): p. F128-133.

52. Couser, R.J., T.B. Ferrara, J. Ebert, R.E. Hoekstra, and J.J. Fangman, *Effects of exogenous surfactant therapy on dynamic compliance during mechanical breathing in preterm infants with hyaline membrane disease.* J Pediatr, 1990. **116**(1): p. 119-124.

53. Suresh, G.K. and R.F. Soll, *Overview of surfactant replacement trials.* J Perinatol, 2005. **25 Suppl 2**: p. S40-44.

54. Kulkarni, R.M., A. Herman, M. Ikegami, J.M. Greenberg, and A.L. Akeson, *Lymphatic ontogeny and effect of hypoplasia in developing lung.* Mechanisms of Development, 2011. **128**(1): p. 29-40.

55. Reed, H.O., L. Wang, J. Sonett, M. Chen, J. Yang, L. Li, P. Aradi, Z. Jakus, J. D'Armiento, W.W. Hancock, and M.L. Kahn, *Lymphatic impairment leads to pulmonary tertiary lymphoid organ formation and alveolar damage.* J Clin Invest, 2019. **129**(6): p. 2514-2526.

56. Viemari, J.C., H. Burnet, M. Bévengut, and G. Hilaire, *Perinatal maturation of the mouse respiratory rhythm-generator: in vivo and in vitro studies.* Eur. J. Neurosci., 2003. **17**(6): p. 1233-1244.

57. Thoby-Brisson, M., J.B. Trinh, J. Champagnat, and G. Fortin, *Emergence of the pre-Bötzinger respiratory rhythm generator in the mouse embryo.* J. Neurosci., 2005. **25**(17): p. 4307-4318.

58. Niblock, M.M., A. Perez, S. Broitman, B. Jacoby, E. Aviv, and S. Gilkey, *In utero development of fetal breathing movements in C57BL6 mice.* Respir Physiol Neurobiol, 2020. **271**: p. 103288.

59. Jia, W., H. Hitchcock-Szilagyi, W. He, J. Goldman, and F. Zhao, *Engineering the Lymphatic Network: A Solution to Lymphedema.* Advanced Healthcare Materials, 2021. **10**(6): p. 2001537.

60. Lagassé, H.A., A. Alexaki, V.L. Simhadri, N.H. Katagiri, W. Jankowski, Z.E. Sauna, and C. Kimchi-Sarfaty, *Recent advances in (therapeutic protein) drug development.* F1000Res, 2017. **6**: p. 113.

61. Szuba, A., M. Skobe, M.J. Karkkainen, W.S. Shin, D.P. Beynet, N.B. Rockson, N. Dakhil, S. Spilman, M.L. Goris, H.W. Strauss, T. Quertermous, K. Alitalo, and S.G. Rockson, *Therapeutic lymphangiogenesis with human recombinant VEGF-C.* FASEB J., 2002. **16**(14): p. 1985-1987.

62. Hall, M.A., H. Robinson, W. Chan, and E.M. Sevick-Muraca, *Detection of lymphangiogenesis by near-infrared fluorescence imaging and responses to VEGF-C during healing in a mouse full-dermis thickness wound model.* Wound Repair Regen., 2013. **21**(4): p. 604-615.

63. Zhou, H., M. Wang, C. Hou, X. Jin, and X. Wu, *Exogenous VEGF-C Augments the Efficacy of Therapeutic Lymphangiogenesis Induced by Allogenic Bone Marrow Stromal Cells in a Rabbit Model of Limb Secondary Lymphedema.* Jpn. J. Clin. Oncol., 2011. **41**(7): p. 841-846.

64. Jin, D.P., A. An, J. Liu, K. Nakamura, and S.G. Rockson, *Therapeutic Responses to Exogenous VEGF-C Administration in Experimental Lymphedema: Immunohistochemical and Molecular Characterization.* Lymphat. Res. Biol., 2009. **7**(1): p. 47-57.

65. Alitalo, K., *The lymphatic vasculature in disease.* Nat. Med., 2011. **17**(11): p. 1371-1380.

66. Tammela, T., A. Saaristo, T. Holopainen, J. Lyytikkä, A. Kotronen, M. Pitkonen, U. Abo-Ramadan, S. Ylä-Herttuala, T.V. Petrova, and K. Alitalo, *Therapeutic differentiation and maturation of lymphatic vessels after lymph node dissection and transplantation.* Nat. Med., 2007. **13**(12): p. 1458-1466.

67. Lähteenvuo, M., K. Honkonen, T. Tervala, T. Tammela, E. Suominen, J. Lähteenvuo, I. Kholová, K. Alitalo, S. Ylä-Herttuala, and A. Saaristo, *Growth Factor Therapy and Autologous Lymph Node Transfer in Lymphedema.* Circulation, 2011. **123**(6): p. 613-620.

68. Visuri, M.T., K.M. Honkonen, P. Hartiala, T.V. Tervala, P.J. Halonen, H. Junkkari, N. Knuutinen, S. Yla-Herttuala, K.K. Alitalo, and A.M. Saarikko, *VEGF-C and VEGF-C156S in the pro-lymphangiogenic growth factor therapy of lymphedema: a large animal study.* Angiogenesis, 2015. **18**(3): p. 313-326.

69. Norrmén, C., T. Tammela, T.V. Petrova, and K. Alitalo, *Biological Basis of Therapeutic Lymphangiogenesis.* Circulation, 2011. **123**(12): p. 1335-1351.

70. Enholm, B., T. Karpanen, M. Jeltsch, H. Kubo, F. Stenback, R. Prevo, D.G. Jackson, S. Yla-Herttuala, and K. Alitalo, *Adenoviral expression of vascular endothelial growth factor-C induces lymphangiogenesis in the skin.* Circ. Res., 2001. **88**(6): p. 623-629.

71. Saaristo, A., T. Veikkola, T. Tammela, B. Enholm, M.J. Karkkainen, K. Pajusola, H. Bueler, S. Ylä-Herttuala, and K. Alitalo, *Lymphangiogenic gene therapy with minimal blood vascular side effects.* J. Exp. Med., 2002. **196**(6): p. 719-730.

72. Karkkainen, M.J., A. Saaristo, L. Jussila, K.A. Karila, E.C. Lawrence, K. Pajusola, H. Bueler, A. Eichmann, R. Kauppinen, M.I. Kettunen, S. Ylä-Herttuala, D.N. Finegold, R.E. Ferrell, and K. Alitalo, *A model for gene therapy of human hereditary lymphedema.* Proceedings of the National Academy of Sciences, 2001. **98**(22): p. 12677-12682.

73. Saaristo, A., T. Tammela, J. Timonen, S. Yla-Herttuala, E. Tukiainen, S. Asko-Seljavaara, and K. Alitalo, *Vascular endothelial growth factor-C gene therapy restores lymphatic flow across incision wounds.* The FASEB Journal, 2004. **18**(14): p. 1707-1709.

74. Hollevoet, K. and P.J. Declerck, *State of play and clinical prospects of antibody gene transfer.* J. Transl. Med., 2017. **15**(1): p. 131.

75. Nault, J.C., S. Datta, S. Imbeaud, A. Franconi, M. Mallet, G. Couchy, E. Letouzé, C. Pilati, B. Verret, J.F. Blanc, C. Balabaud, J. Calderaro, A. Laurent, M. Letexier, P. Bioulac-Sage, F. Calvo, and J. Zucman-Rossi, *Recurrent AAV2-related insertional mutagenesis in human hepatocellular carcinomas.* Nat. Genet., 2015. **47**(10): p. 1187-1193.

76. Laczko, D., M.J. Hogan, S.A. Toulmin, P. Hicks, K. Lederer, B.T. Gaudette, D. Castano, F. Amanat, H. Muramatsu, T.H. Oguin, 3rd, A. Ojha, L. Zhang, Z. Mu, R. Parks, T.B. Manzoni, B. Roper, S. Strohmeier, I. Tombacz, L. Arwood, R. Nachbagauer, K. Kariko, J. Greenhouse, L. Pessaint, M. Porto, T. Putman-Taylor, A. Strasbaugh, T.A. Campbell, P.J.C. Lin, Y.K. Tam, G.D. Sempowski, M. Farzan, H. Choe, K.O. Saunders, B.F. Haynes, H. Andersen, L.C. Eisenlohr, D. Weissman, F. Krammer, P. Bates, D. Allman, M. Locci, and N. Pardi, *A Single Immunization with Nucleoside-Modified mRNA Vaccines Elicits Strong Cellular and Humoral Immune Responses against SARS-CoV-2 in Mice.* Immunity, 2020. 13;53(4): p. 724-732.

77. Pardi, N., M.J. Hogan, F.W. Porter, and D. Weissman, *mRNA vaccines - a new era in vaccinology.* Nat Rev Drug Discov, 2018. **17**(4): p. 261-279.

78. Pardi, N., M.J. Hogan, R.S. Pelc, H. Muramatsu, H. Andersen, C.R. DeMaso, K.A. Dowd, L.L. Sutherland, R.M. Scearce, R. Parks, W. Wagner, A. Granados, J. Greenhouse, M. Walker, E. Willis, J.S. Yu, C.E. McGee, G.D. Sempowski, B.L. Mui, Y.K. Tam, Y.J. Huang, D. Vanlandingham, V.M. Holmes, H. Balachandran, S. Sahu, M. Lifton, S. Higgs, S.E. Hensley, T.D. Madden, M.J. Hope, K. Kariko, S. Santra, B.S. Graham, M.G. Lewis,

T.C. Pierson, B.F. Haynes, and D. Weissman, *Zika virus protection by a single low-dose nucleoside-modified mRNA vaccination.* Nature, 2017. **543**(7644): p. 248-251.

79. Pardi, N., A.J. Secreto, X. Shan, F. Debonera, J. Glover, Y. Yi, H. Muramatsu, H. Ni, B.L. Mui, Y.K. Tam, F. Shaheen, R.G. Collman, K. Kariko, G.A. Danet-Desnoyers, T.D. Madden, M.J. Hope, and D. Weissman, *Administration of nucleoside-modified mRNA encoding broadly neutralizing antibody protects humanized mice from HIV-1 challenge.* Nat Commun, 2017. **8**: p. 14630.

80. Kranz, L.M., M. Diken, H. Haas, S. Kreiter, C. Loquai, K.C. Reuter, M. Meng, D. Fritz, F. Vascotto, H. Hefesha, C. Grunwitz, M. Vormehr, Y. Hüsemann, A. Selmi, A.N. Kuhn, J. Buck, E. Derhovanessian, R. Rae, S. Attig, J. Diekmann, R.A. Jabulowsky, S. Heesch, J. Hassel, P. Langguth, S. Grabbe, C. Huber, Ö. Türeci, and U. Sahin, *Systemic RNA delivery to dendritic cells exploits antiviral defence for cancer immunotherapy.* Nature, 2016. **534**(7607): p. 396-401.

81. Petsch, B., M. Schnee, A.B. Vogel, E. Lange, B. Hoffmann, D. Voss, T. Schlake, A. Thess, K.J. Kallen, L. Stitz, and T. Kramps, *Protective efficacy of in vitro synthesized, specific mRNA vaccines against influenza A virus infection.* Nat Biotechnol, 2012. **30**(12): p. 1210-1216.

82. Alberer, M., U. Gnad-Vogt, H.S. Hong, K.T. Mehr, L. Backert, G. Finak, R. Gottardo, M.A. Bica, A. Garofano, S.D. Koch, M. Fotin-Mleczek, I. Hoerr, R. Clemens, and F. von Sonnenburg, *Safety and immunogenicity of a mRNA rabies vaccine in healthy adults: an open-label, non-randomised, prospective, first-in-human phase 1 clinical trial.* Lancet, 2017. **390**(10101): p. 1511-1520.

83. Jackson, L.A., E.J. Anderson, N.G. Rouphael, P.C. Roberts, M. Makhene, R.N. Coler, M.P. McCullough, J.D. Chappell, M.R. Denison, L.J. Stevens, A.J. Pruijssers, A. McDermott, B. Flach, N.A. Doria-Rose, K.S. Corbett, K.M. Morabito, S. O'Dell, S.D. Schmidt, P.A. Swanson, 2nd, M. Padilla, J.R. Mascola, K.M. Neuzil, H. Bennett, W. Sun, E. Peters, M. Makowski, J. Albert, K. Cross, W. Buchanan, R. Pikaart-Tautges, J.E. Ledgerwood, B.S. Graham, J.H. Beigel, and R.N.A.S.G. m, *An mRNA Vaccine against SARS-CoV-2 - Preliminary Report.* N Engl J Med, 2020. 383;20: p. 1920-1931

84. Mulligan, M.J., K.E. Lyke, N. Kitchin, J. Absalon, A. Gurtman, S. Lockhart, K. Neuzil, V. Raabe, R. Bailey, K.A. Swanson, P. Li, K. Koury, W. Kalina, D. Cooper, C.

Fontes-Garfias, P.Y. Shi, O. Tureci, K.R. Tompkins, E.E. Walsh, R. Frenck, A.R. Falsey, P.R. Dormitzer, W.C. Gruber, U. Sahin, and K.U. Jansen, *Phase I/II study of COVID-19 RNA vaccine BNT162b1 in adults.* Nature, 2020. Vol 586: p. 589-593

85. Bialkowski, L., A. van Weijnen, K. Van der Jeught, D. Renmans, L. Daszkiewicz, C. Heirman, G. Stangé, K. Breckpot, J.L. Aerts, and K. Thielemans, *Intralymphatic mRNA vaccine induces CD8 T-cell responses that inhibit the growth of mucosally located tumours.* Sci Rep, 2016. **6**: p. 22509.

86. Pardi, N., S. Tuyishime, H. Muramatsu, K. Kariko, B.L. Mui, Y.K. Tam, T.D. Madden, M.J. Hope, and D. Weissman, *Expression kinetics of nucleoside-modified mRNA delivered in lipid nanoparticles to mice by various routes.* J Control Release, 2015. **217**: p. 345-51.

87. Magadum, A., K. Kaur, and L. Zangi, *mRNA-Based Protein Replacement Therapy for the Heart.* Mol Ther, 2019. **27**(4): p. 785-793.

88. Trepotec, Z., E. Lichtenegger, C. Plank, M.K. Aneja, and C. Rudolph, *Delivery of mRNA Therapeutics for the Treatment of Hepatic Diseases.* Mol Ther, 2019. **27**(4): p. 794-802.

89. Sahu, I., A. Haque, B. Weidensee, P. Weinmann, and M.S.D. Kormann, *Recent Developments in mRNA-Based Protein Supplementation Therapy to Target Lung Diseases.* Mol Ther, 2019. **27**(4): p. 803-823.

90. Zhang, H.X., Y. Zhang, and H. Yin, *Genome Editing with mRNA Encoding ZFN, TALEN, and Cas9.* Mol Ther, 2019. **27**(4): p. 735-746.

91. Perlman, M., J. Williams, and M. Hirsch, *Neonatal pulmonary hypoplasia after prolonged leakage of amniotic fluid.* Arch Dis Child, 1976. **51**(5): p. 349-353.

92. Wigglesworth, J.S. and R. Desai, *Is fetal respiratory function a major determinant of perinatal survival?* Lancet, 1982. **1**(8266): p. 264-267.

93. Moessinger, A.C., R. Harding, T.M. Adamson, M. Singh, and G.T. Kiu, *Role of lung fluid volume in growth and maturation of the fetal sheep lung.* J Clin Invest, 1990. **86**(4): p. 1270-1277.

94. Harding, R. and S.B. Hooper, *Regulation of lung expansion and lung growth before birth.* J Appl Physiol (1985), 1996. **81**(1): p. 209-224.

95. Kitterman, J.A., *The effects of mechanical forces on fetal lung growth.* Clin Perinatol, 1996. **23**(4): p. 727-740.

96. Fewell, J.E., C.C. Lee, and J.A. Kitterman, *Effects of phrenic nerve section on the respiratory system of fetal lambs.* J Appl Physiol Respir Environ Exerc Physiol, 1981. **51**(2): p. 293-297.

97. Liggins, G.C., G.A. Vilos, G.A. Campos, J.A. Kitterman, and C.H. Lee, *The effect of spinal cord transection on lung development in fetal sheep.* J Dev Physiol, 1981. **3**(4): p. 267-274.

98. Bamford, O.S., A. Rivera, T. Tadalan, and W. Ellis, *Effects of in utero phrenic nerve section on the development of collagen and elastin in lamb lungs.* Am Rev Respir Dis, 1992. **146**(5 Pt 1): p. 1202-1205.

99. Sandler, D.L., D.J. Burchfield, J.A. McCarthy, A.M. Rojiani, and W.H. Drummond, *Early-onset respiratory failure caused by severe congenital neuromuscular disease.* J Pediatr, 1994. **124**(4): p. 636-638.

100. Tseng, B.S., S.T. Cavin, F.W. Booth, E.N. Olson, M.C. Marin, T.J. McDonnell, and I.J. Butler, *Pulmonary hypoplasia in the myogenin null mouse embryo.* Am J Respir Cell Mol Biol, 2000. **22**(3): p. 304-315.

101. Maby-El Hajjami, H. and T.V. Petrova, *Developmental and pathological lymphangiogenesis: from models to human disease.* Histochem Cell Biol, 2008. **130**(6): p. 1063-1078.

102. Hanada, T., S. Weitzer, B. Mair, C. Bernreuther, B.J. Wainger, J. Ichida, R. Hanada, M. Orthofer, S.J. Cronin, V. Komnenovic, A. Minis, F. Sato, H. Mimata, A. Yoshimura, I. Tamir, J. Rainer, R. Kofler, A. Yaron, K.C. Eggan, C.J. Woolf, M. Glatzel, R. Herbst, J. Martinez, and J.M. Penninger, *CLP1 links tRNA metabolism to progressive motor-neuron loss.* Nature, 2013. **495**(7442): p. 474-480.

103. Hollevoet, K. and P.J. Declerck, *State of play and clinical prospects of antibody gene transfer.* J Transl Med, 2017. **15**(1): p. 131.

104. Kholova, I., S. Koota, N. Kaskenpaa, P. Leppanen, J. Narvainen, M. Kavec, T.T. Rissanen, T. Hazes, P. Korpisalo, O. Grohn, and S. Yla-Herttuala, *Adenovirus-mediated*

gene transfer of human vascular endothelial growth factor-d induces transient angiogenic effects in mouse hind limb muscle. Hum Gene Ther, 2007. **18**(3): p. 232-244.

105. Sahin, U., K. Kariko, and O. Tureci, *mRNA-based therapeutics--developing a new class of drugs.* Nat Rev Drug Discov, 2014. **13**(10): p. 759-780.

106. Polack, F.P., S.J. Thomas, N. Kitchin, J. Absalon, A. Gurtman, S. Lockhart, J.L. Perez, G. Pérez Marc, E.D. Moreira, C. Zerbini, R. Bailey, K.A. Swanson, S. Roychoudhury, K. Koury, P. Li, W.V. Kalina, D. Cooper, R.W. Frenck, L.L. Hammitt, Ö. Türeci, H. Nell, A. Schaefer, S. Ünal, D.B. Tresnan, S. Mather, P.R. Dormitzer, U. Şahin, K.U. Jansen, and W.C. Gruber, *Safety and Efficacy of the BNT162b2 mRNA Covid-19 Vaccine.* New England Journal of Medicine, 2020. **383**(27): p. 2603-2615.

107. Baden, L.R., H.M. El Sahly, B. Essink, K. Kotloff, S. Frey, R. Novak, D. Diemert, S.A. Spector, N. Rouphael, C.B. Creech, J. McGettigan, S. Khetan, N. Segall, J. Solis, A. Brosz, C. Fierro, H. Schwartz, K. Neuzil, L. Corey, P. Gilbert, H. Janes, D. Follmann, M. Marovich, J. Mascola, L. Polakowski, J. Ledgerwood, B.S. Graham, H. Bennett, R. Pajon, C. Knightly, B. Leav, W. Deng, H. Zhou, S. Han, M. Ivarsson, J. Miller, and T. Zaks, *Efficacy and Safety of the mRNA-1273 SARS-CoV-2 Vaccine.* New England Journal of Medicine, 2020. **384**(5): p. 403-416.

108. Rissanen, T.T., J.E. Markkanen, M. Gruchala, T. Heikura, A. Puranen, M.I. Kettunen, I. Kholova, R.A. Kauppinen, M.G. Achen, S.A. Stacker, K. Alitalo, and S. Yla-Herttuala, *VEGF-D is the strongest angiogenic and lymphangiogenic effector among VEGFs delivered into skeletal muscle via adenoviruses.* Circ Res, 2003. **92**(10): p. 1098-1106.

109. Saaristo, A., T. Tammela, A. Farkkila, M. Karkkainen, E. Suominen, S. Yla-Herttuala, and K. Alitalo, *Vascular endothelial growth factor-C accelerates diabetic wound healing.* Am J Pathol, 2006. **169**(3): p. 1080-1087.

110. Skobe, M., T. Hawighorst, D.G. Jackson, R. Prevo, L. Janes, P. Velasco, L. Riccardi, K. Alitalo, K. Claffey, and M. Detmar, *Induction of tumor lymphangiogenesis by VEGF-C promotes breast cancer metastasis.* Nat Med, 2001. **7**(2): p. 192-198.

111. Hartiala, P., S. Suominen, E. Suominen, I. Kaartinen, J. Kiiski, T. Viitanen, K. Alitalo, and A.M. Saarikko, *Phase 1 Lymfactin(®) Study: Short-term Safety of Combined*

Adenoviral VEGF-C and Lymph Node Transfer Treatment for Upper Extremity Lymphedema. J Plast Reconstr Aesthet Surg, 2020. **73**(9): p. 1612-1621.

112. Brown, S.D., D. Zurakowski, D.P. Rodriguez, P.S. Dunning, R.J. Hurley, and G.A. Taylor, *Ultrasound diagnosis of mouse pregnancy and gestational staging.* Comp Med, 2006. **56**(4): p. 262-271.

8. Bibliography of the candidate's publications

I. Szőke, D., Kovács G., Kemecsei, É., Bálint, L., Szoták-Ajtay, K., Aradi, P., Styevkóné Dinnyés, A., Mui, B.L., Tam, Y.K., Madden, T.D., Karikó, K., Kataru, R.P., Hope, M.J., Weissman, D., Mehrara, B.J., Pardi, N., and Jakus, Z. (2021)

Nucleoside-modified VEGFC mRNA induces organ-specific lymphatic growth and reverses experimental lymphedema.

Nat Commun. 2021, 12, 3460. p. 1-18. https://doi.org/10.1038/s41467-021-23546-6

Impact Factor: 17.694

II. Szoták-Ajtay, K., Szőke, D., Kovács, G., Andréka, J., Brenner, GB., Giricz, Z., Penninger, J., Kahn, ML. and Jakus, Z. (2020)

Reduced Prenatal Pulmonary Lymphatic Function Is Observed in Clp1K/K Embryos with Impaired Motor Functions Including Fetal Breathing Movements in Preparation of the Developing Lung for Inflation at Birth.

Front. Bioeng. Biotechnol. 2020, 8:136. p. 1-15. https://doi.org/10.3389/fbioe.2020.00136

Impact Factor: 5.890

10. Acknowledgements

Firstly, I am deeply grateful to my supervisor Dr. Zoltán Jakus for his assistance and support at every stage of the research project.

I would like to express my sincere gratitude to all the lab members for the technical assistance and support, namely: Carolin Christ, Éva Kemecsei, Dr. Gábor Kovács, Kitti Szoták-Ajtay, Dr. László Bálint, Petra Aradi, Valéria Németh and Dr. Zsombor Ocskay.

I would like to express my appreciation to the whole Department of Physiology, Semmelweis University.

I would like to offer my special thanks to Dr. Norbert Pardi for intellectual support and production of the VEGFC mRNA-LNPs.

I thank Dr. Babak J. Mehrara for the lymphedema mouse model.

I would like to thank to the supporters. This work was supported by the Lendület program of the Hungarian Academy of Sciences (LP2014-4/2019 to Dr. Zoltán Jakus), the National Research, Development and Innovation Office (NVKP_16-2016-1-0039 to Dr. Zoltán Jakus), the European Union and the Hungarian Government (VEKOP-2.3.2-16-2016-00002 to Dr. Zoltán Jakus, EFOP-3.6.3-VEKOP-16-2017-00009 and ÚNKP-21-4-1 to Dr. Dániel Szőke) and the Higher Education Institutional Excellence Program of the Ministry for Innovation and Technology in Hungary, within the framework of the Molecular Biology thematic program of the Semmelweis University.

Finally, I would like to express my gratitude to my wife and parents. Without their encouragement and mental support, I would not be the person I am today, and it would have been impossible for me to complete my study.